Geochemical evidence for garnet eclogite melts in Lena Trough MORB (Arctic Ocean)

François Nauret[1,*], Jonathan E. Snow[1,‡]

[1] Max-Planck Institut für Chemie
Postfach 3060
55122 Mainz, Germany

* Present Address:
Institut de Physique du Globe,

4 place Jussieu - 75252 Paris cedex 05
Localisation : Tour 14, 3e étage, Aile 14-15, France.
E-mail: nauret@ipgp.jussieu.fr

‡ Present Address:
Department of Geosciences
University of Houston
Houston, TX 77204-5007 USA

Correponding author:
J.E. Snow. Department of Geosciences, University of Houston
Houston, TX 77204-5007 USA
E-mail: jesnow@uh.edu
Tel: 713/743-5312
Fax: 713/748-7906

ABSTRACT

The composition of the MORB (Mid-Ocean Ridge Basalt) mantle source has been debated over several decades in order to examine whether apparently garnet bearing sources represent deep partial melting or selective melting of garnet-bearing pyroxenite veins. The degree of pyroxenite contribution depends on the presence of pyroxenite in MORB sources and on the degree of partial melting, whereby lower degrees of melting increase the pyroxenitic source contribution. Here we report major and trace element compositions of melt generated at the ultraslow spreading Lena Trough (Arctic Ocean). Lena trough is characterized by predominantly peridotite outcrop except for minor basalts at its northern end and in its south-central region. The northern LenaTrough and western Gakkel Ridge basalts are normal MORB. In the Central Lena Trough, alkali basalts with relatively high Mg# (Mg# 60-65) are characterized by high SiO_2 (51.06-51.65 wt%), Al_2O_3 (18.10-18.44 wt%), Na_2O (4.0-4.2 wt%), K_2O(1.00-1.57), K_2O/TiO_2 (0.63-0.89), $(La/Sm)_{PM}$ (1.4-1.8) and low FeO (6.52-6.80 wt%) contents. Based on these characteristics, they are interpreted as primitive (despite MgO of 5.0 to 6.5 wt%) low degree shallow partial melts. However, they also display a clear garnet signature with low HREE content, relative to MREE ($(Dy/Yb)_{PM}$=1.20-1.32). . Using major and trace elements, we demonstrate that the fertile component observed in the Central Lena Trough melts cannot be a derived from peridotite partial melting but rather from a pyroxenite. In addition, we show that melt compositions from the central part of Lena Trough to the westernmost Gakkel Ridge, are related by a binary mixing relationship, involving a spinel peridotite source and a pyroxenite.

1 INTRODUCTION

The distribution of incompatible element enriched components in the mantle has been at issue for some time [1]. On the one hand many have argued for a relatively homogeneous distribution of geochemical anomalies within an otherwise relatively homogeneous mantle, which is in chemical equilibrium on a relatively large scale [2]. On the other hand, basalts from Ocean Islands, and in some cases from mid-ocean ridges, show mixing trends that indicate mixing between very distinct reservoirs, even when those reservoirs are persistent over a wide region [3]. These can best be explained by mixing between an early melting fraction that mixes with melts derived from the main phase of silicate melting at a relatively high level in the crust [4]. Studies of peridotites from the SW Indian Ridge have delivered some evidence in favor of such a theory. In the two studies to date, both found peridotite clinopyroxene compositions that indicated a degree of disequilibrium between the peridotites and the melts sampled nearby [5, 6]. Both of these lines of evidence seem to suggest that a low-melting component derived from hydrous mantle veins is a major source of enriched material to mid-ocean ridges. As most of the heat-producing elements in the mantle are strongly lithophilic, these enriched regions form a major part of the radiogenic internal heating of the mantle, a major repository of water, and are potentially derived from deep subduction of crustal material.

However, in all of the preceding studies, melts derived from a supposed vein source have comprised only a small component of basalt magmatic series that otherwise

could easily be generated by the partial melting of peridotite. Secondly, though pyroxenite veins in peridotite massifs worldwide are commonplace, the vein assemblages observed generally crosscut features related to or postdating melting. If these pyroxenite veins at one time had been mantle veins in the asthenosphere, then they would have melted during emplacement beneath the ridge and been lost. Even this type of pyroxenite vein is relatively rare in peridotites dredged from the ocean floor. Thus, the evidence for mantle veins is ambiguous at best, and the vast majority of mid-ocean ridge basalts could be generated either by pure peridotite partial melting or by the contribution of a garnet-bearing component form a vein source.

The natural place to look for such melts is at an ultra slow spreading mid-ocean ridge. There, the degree of melting in the mantle is depressed by the thick overlying lithosphere, resulting in a relatively thin crust [7-9] and thus a higher proportion of vein-derived material in the source of the basalts generated there. For this reason, the cruise ARK-XX/2 of the PFS Polarstern (Alfred Wegener Institute for Polar and Marine Research, Bremerhaven, Germany) was undertaken in the summer of 2004. The object of this cruise was the Lena Trough, an obliquely spreading segment of the North American-Eurasian plate boundary that connects the Knipovitch and Gakkel Ridges. The spreading rate between the two plates in this region is one of the slowest in the world (13 mm/yr full rate), and thus the degree of partial melting in the mantle should be depressed. Preliminary indications from neighboring Gakkel Ridge indicated that this was so [10, 11]. An additional consideration at Lena Trough is its obliquity: Lena Trough spreads at a 55° angle to the direction of the rift valley of the orthogonal Gakkel Ridge to the north. This

obliquity should result in an additional cooling and thickening of the lithosphere, and thus a further lowered degree of partial melting in the mantle [12, 13], reducing the effective spreading rate to just 7 mm/yr, lower than that on any mid-ocean ridge in the world. Sampling on Lena Trough produced mostly mantle peridotite, with basalt recovered in only three dredge hauls in a restricted area **[14]**.

2 SAMPLES AND ANALYTICAL PROCEDURE

2.1 *Samples*

Dredge locations containing volcanic rocks are shown in Fig. 1 (Table 1). Glassy pillow basalt samples were collected in three areas: Central Lena Trough with dredges PS66-261, 262, PS55-90, Northern Lena Trough with dredges PS66-219, 217, HLY0102-D8 and D11, and westernmost Gakkel Ridge with dredges PS59-216, 218,221, 223 and PS66-214 (Table 1). Basalt type, discriminated based on the mineralogy is either plagioclase or olivine phyric or plagioclase-olivine phyric or aphyric. The sample groundmass is mainly composed of plagioclase, olivine and clinopyroxene microlites in a glassy matrix. A major difference between these basalts is the amount of vesicles. Westernmost Gakkel Ridge MORB and Northern Lena Trough basalts display only a low percent of vesicles (<1 to 5%). In contrast, basalts collected in southern part of Lena Trough are very vesicular (up to 25%) despite water depths of over 3500m.

2.2 Analytical procedure

Major element compositions were analyzed with a JEOL Super probe 8200 electron microprobe and trace element compositions by LA-ICP-MS, both at the Max Planck Institut fűr Chemie (Mainz). All analyses were done on hand picked glass chips mounted in an epoxy ring. Major and trace element compositions were measured on the same chip. Major element analysis were performed using 20 kV accelerating voltage with a 2 μm diameter beam. VG-2 was used as standard in order to control the quality of the acquisition. Average of repeated measurement of VG-2 is reported in Table 1. The reported analysis is the average of at least three different runs. For trace elements, LA-ICP-MS analyses were done with a 120 μm diameter beam, at a laser power of 2.5J/cm^2, repetition rate of 10Hz, energy output 80%, dwell time per peak 120ms, RF power 1275W and Ar and He flows of 0.85 and 0.65l/min respectively. NIST 612 and KL2-G were used to establish working curves for each element. The quality of the data was controlled by repeated measurement of ATHO-G reference glass (Table 2). Reported sample composition is an average of at least three runs done, for each sample, in a single glass chip.

3 RESULTS

3.1 Major Elements

The 17 Samples (N=17) from the central part of Lena Trough are enriched alkali basalt having MgO from 5.05 to 6.48 weight %, SiO_2 from 51.1 to 51.8, high Al_2O_3 from 18.10 to 18.44, Na_2O from 4.00 to 4.29, very high K_2O from 1.00 to 1.98, TiO_2 from 1.55

to 2.22 and low FeO* from 6.52 to 6.79 (Fig. 3). Their Mg# [molar Mg/(Mg + Fe^{2+})] ranges from 0.60 to 0.66. They are *ne*-normative and plot at the border between trachy-basalt and basaltic trachy-andesite fields in a standard Na_2O+K_2O versus SiO_2 (TAS) plot [15] (Fig.2). They are among the most alkali-rich samples ever dredged from a mid-ocean ridge. Only one sample from South West Indian Ridge presents similar very high Na_2O+K_2O [4] (Fig. 2). Samples (N=32) from westernmost Gakkel Ridge and Northern Lena Trough have more typical MORB compositions. They have MgO from 6.63 to 8.24, SiO_2 from 49.41 to 51.03, Al_2O_3 from 15.42 to 17.45, Na_2O from 2.94 to 3.54, K_2O from 0.07 to 0.66 and FeO* from 8.94 to 10.32 (Table 2 and Fig. 3). The Mg# is nearly constant (0.57-0.65). Sample 219-2 has a somewhat similar major element composition to those of Central Lena Trough basalts with higher Al_2O_3 and K_2O/TiO_2 than westernmost Gakkel Ridge-Northern Lena Trough, but with lower SiO_2 (Fig. 3). It is *ne*-normative like the central Lena samples, whereas all of the other northern Lena Trough samples are *hy*-normative and plot in the basalt field of the TAS diagram (Fig 2).

Plotted against MgO, The central Lena Trough basalts have constant SiO_2-Na_2O-FeO*-Al_2O_3 compositions. They show a positive correlation with CaO and negative correlation with K_2O/TiO_2 (Fig. 3). Samples from the westernmost Gakkel Ridge-Northern Lena Trough show a broadly negative Na_2O-MgO correlation, positive CaO-MgO correlation and nearly constant FeO, and K_2O/TiO_2 composition against MgO (Fig.3). The scatter shown by westernmost Gakkel Ridge-Northern Lena Trough samples in SiO_2-Al_2O_3 vs. MgO is mainly due to sample 219-2 and HLY0102-D8-17. Central Lena Trough lavas have lower MgO than Northern Lena Trough (Fig. 3). However they have a significantly

higher K_2O content and K_2O/TiO_2 than westernmost Gakkel Ridge -Northern Lena Trough (Fig. 3) basalts for a given Mg#.

Sodium and iron content normalized to a common value of magnesium, to correct for low-pressure crystallization, may yield information about the conditions of source melting [16, 17]. For these samples, correction of major element composition to an MgO of 8 wt% uses a linear liquid line of descent (LLD). $Fe_{8.0}$ values are often used as a proxy for depth of melting and $Na_{8.0}$ values as a proxy for the degree of partial melting. Central Lena Trough samples have $Fe_{8.0}$ and $Na_{8.0}$ values of 4.2 and 6.4, respectively. These apparent values are reported in Fig. 4. The term "apparent" is used because the MgO normalization assumes here that all primitive MORB have 8 wt.% MgO. In alkalic rocks, primary melts may have significantly lower MgO [18]. In this diagram, Central Lena Trough samples appear to plot at an extremity of the global correlation. This is unchanged if they are assumed to be primitive melts and are plotted using their uncorrected compositions. Westernmost Gakkel Ridge-Northern Lena Trough samples have $Fe_{8.0}$ and $Na_{8.0}$ values of 10.31 and 3.00, respectively [calculations are done with samples having MgO higher than 7 wt%] (Fig. 4). They plot also in this global correlation and these values are higher than these from Gakkel ridge MORB described by [19] (Fig. 4).

3.2 Trace elements

Central Lena Trough basalts are extremely enriched in all incompatible trace elements, with high La/Sm (2.3-2.8), high Ba/Th and Nb/U (350 to386, and 69 to 74), high

$(Dy/Yb)_{PM}$ ratio (1.2 to 1.3) (Fig. 5 and 8). They have strong negative Th and U anomalies and positive Nb, Sr, Zr Hf anomalies (Fig. 5). They have also positive Eu/Eu* ratios (1.00 to 1.08) (Fig. 7-c and d). Moreover, they have very unusual trace element ratios compared to N-MORB, with very low Ba/Rb (9.4±0.4) and Nb/Ta (14.6± 0.5) ratios and very high Nb/U ratios. Although they have very low Ba/Rb ratio, they are very fresh looking under binocular observation and thus do not seem to be affected by seawater alteration.

Westernmost Gakkel Ridge-Northern Lena Trough basalts display more trace element compositional variation than Central Lena Trough (Fig. 5). Excluding sample PS66:219-2, they have Ba/Th ratio ranging from 117 to 256 with Ba/Rb (11.8± 1.8) and Nb/U ratio (48.6± 10.9) similar to N-MORB reference value (11.4± 0.2 and 47± 10, respectively [20]), and finally Nb/Ta=14.9± 1.3 (Fig. 8). In addition, they have relatively low Nd/Pb (19.8±1.9). Averaged La/Sm is 1.13± 0.25 and the MREE to HREE trace element pattern is flat and $(Dy/Yb)_{PM}$ is 1.10± 0.03 (Fig. 8). Eu/Eu* ratio is lower than 1 (0.95± 0.05) (Fig. 6-c and d). The sample 219-2 is different with higher La/Sm, $(Dy/Yb)_{PM}$ and Eu/Eu* (1.6, 1.19 and 1.01 respectively) and Nb/Ta and Nb/U (13.7 and 48.5 respectively). This sample shares common trace element characteristics with the Central Lena Trough basalts (Fig. 5 and 7-c- d and Fig. 8).

4 DISCUSSION

4.1 Fractional crystallization

Mid-ocean ridge rocks are commonly affected by fractional crystallization of olivine, which increases incompatible-element abundances while lowering MgO contents. Plagioclase fractionation commonly also affects these rocks, which produces Eu anomalies due to the relatively high partition coefficient of divalent Eu in plagioclase. Strontium has an even higher partition coefficient than Eu in plagioclase, whereas in other minerals relevant to basalt genesis, such as clinopyroxene, the partition coefficient of Sr is similar to that of Nd. Consequently, testing for negative or positive Eu anomalies and for corresponding Sr/Nd ratios can shows any plagioclase crystallization effect. This is illustrated in Fig 7, with several diagrams: Y and Eu/Eu* versus MgO and Eu/Eu* versus Sr/Nd. Mineralogically, we have observed olivine and plagioclase in the groundmass. We have also observed a small amount of very small phenocrysts of plagioclase and euhedral olivine in the glassy rim for all samples.

Most of the westernmost Gakkel Ridge and northern Lena Trough dredges have relatively homogeneous compositions, except for the PS66-219-2 and HLY01-02-D8-17 samples. The major elements of the northern Lena basalts fall generally (except for Al_2O_3) on liquid lines of descent calculated using MELTS [21] from the most primitive compositions with a plagioclase+olivine crystallization sequence (Fig. 6). First, we notice that lavas from PS66-217, 214, 219 have higher Y at a given MgO compared to other lavas from the same group (Fig. 7). While the high Y lavas do not show a correlation between Y and MgO, other lavas broadly define a negative correlation between Y and MgO (Fig. 7). This correlation is interpreted as reflecting olivine+plagioclase fractionation. Moreover, we clearly observe a positive correlation between Eu/Eu* versus Sr/Nd (Fig

7a-c-d) in these samples. This suggests plagioclase fractionation, consistent with the observation of small plagioclase phenocrysts. Sample 219-2 has a much higher Eu/Eu* (1.07) than other westernmost Gakkel Ridge-northern Lena Trough samples (Fig. 7a-c-d) at a given MgO.

The Central Lena Trough samples show very high and constant Al_2O_3, high Eu/Eu* and $(Sr/Nd)_{PM}$ (1.04 to 1.08 and 1.40 to 1.54, respectively). We observe a positive correlation between both CaO and CaO/Al_2O_3 versus MgO, a negative correlation between Y and MgO but no correlation between Eu/Eu* and Sr/Nd (Fig. 3 and 7a-d). Major element models [21] suggest that plagioclase is the primary liquidus silicate phase under nearly all conceivable conditions. However, from the high Al_2O_3 content of those lavas, we infer that they are not affected by shallow plagioclase fractionation or accumulation. Moreover, there is no correlation between Eu/Eu* and $(Sr/Nd)_{PM}$ (Fig. 7) that might suggest plagioclase fractionation. Thus, the high Eu/Eu* and $(Sr/Nd)_{PM}$ ratios are interpreted as a source characteristic. Given that plagioclase would crystallize first from this magma, the relatively low MgO content (5.0 to 6.5 wt%) is unlikely to be due to olivine fractionation either. Instead of plagioclase, the positive CaO versus MgO correlation might suggest clinopyroxene (Cpx) crystallization, possibly at high pressure. However, the constancy of Sc concentration versus MgO and the high Mg number of the lavas argues against extensive Cpx crystallization (Fig.7-b and Table 2). Instead, negative correlations between K_2O (or K_2O/TiO_2, i.e. used as source proxy) versus MgO, Na_2O or versus La/Sm (not shown) suggest that those compositional variations reflect more the source composition or mixing processes rather than shallow pressure crystallization. Moreover, the central

Lena trough lavas cannot be derived form Northern Lena Trough primitive magmas by any crystal fractionation process (Fig. 6). Major elements Al_2O_3, FeO and K_2O do not permit such an interpretation, nor do any trace elements or trace element ratios.

Thus Central Lena Trough samples have thus not been affected by shallow fractionation of olivine, plagioclase or clinopyroxene, and are nearly primary. Sample PS66-219-2 has a composition intermediate between the central and northern Lena Trough compositions, but does not appear to be a simple combination of linear mixing and fractionation. The Northern Lena/Western Gakkel basalts appear to be more strongly affected by low-pressure crystallization.

4.2 Source composition and simple partial melting

Partial melting conditions (pressure and degree of partial melting) can be estimated by major element compositions of primitive MORB. Whereas SiO_2 and FeO* are proxies for depth of partial melting, the degree of partial melting can be estimated with Na_2O [16, 17]: low SiO_2 and high FeO* content for deep melt generation and high Na_2O for low degree partial melting. In order to illustrate this depth and degree of partial melting effect, we report experimental results [22, 23] done for variable pressure of melting (Fig. 3). In order to examine partial melting conditions, first we look at the source composition. Taking into account the fact that the studied samples were collected along Lena Trough and the westernmost Gakkel Ridge area, we compare them with Mid-Atlantic Ridge (MAR) MORB and experimental studies of partial melting of a peridotite assemblage.

4.2.1 Assuming a peridotite source

If both sets of basalts were derived from a mineralogically similar peridotite source, we may use SiO_2, FeO and Na_2O proxies in order to establish a relative depth and degree of partial melting between the Central Lena Trough and Westernmost Gakkel Ridge-Northern Lena Trough basalts. The Central Lena Trough basalts appear to be generated at shallower pressure and lower degree of partial melting than the Northern Lena Trough, because they have lower FeO, higher SiO_2 and Na_2O (Fig. 9).

Northern Lena Trough and westernmost Gakkel Ridge: in Figure 9, we compare melt compositions with experimental fertile peridotite partial melting results [24]. Most of the northern Lena Trough samples are not primitive (MgO lower than 8 wt%) because they are probably affected by shallow olivine and plagioclase fractionation. Consequently, we mainly focus on the most primitive samples (HLY 0102-D8-17) having SiO_2=49.7, FeO=8.94, Na_2O=2.94 and MgO= 8.24 wt% though this sample has a composition slightly different than other Northern Lena Trough-westernmost Gakkel Ridge lavas. On the SiO_2-FeO* diagram, we observe that samples HLY 0102-D8-17 plot between experimental lines resulting from melting experiment done at 10 kbar and 15 kbar with a fertile spinel peridotite as source [24] (Fig. 9). In a Na_2O-FeO* plot, this HLY 0102-D8-17 composition is intermediate between melt compositions done by 12 and 28% degree partial melting (Fig. 8). Thus, by comparison with those experiments, the northern Lena Trough basalts may be generated by relatively high degree partial melting (>12%), similar to N-MORB [16, 17]. Consequently, we interpret the northern Lena Trough samples as having been generated at around 15 kbar by relatively high degree partial melting

of spinel peridotite, due to their similar trace element characteristics as N-MORB.

Central Lena Trough: These samples are interpreted as to be close to primitive (see above section 4.1) and can be compared directly with peridotite melt experimental results and primitive MORB. Relative to MAR-MORB, Central Lena Trough lavas are clearly distinct in Al_2O_3 and FeO (Fig. 3). The samples have relatively high SiO_2 (51-52 wt%) and high Al_2O_3, Na_2O, K_2O, low CaO, FeO*, MgO and CaO/Al_2O_3 associated with high La/Sm. This is a characteristic for low degree partial melts [25]. Furthermore, they have a much lower FeO content at a given SiO_2 than Northern Lena Trough, suggesting a shallower pressure of melting (Fig. 9).

Next we compare the Central Lena Trough samples to experimental results obtained by low degree partial melting of peridotite [26-29] at relatively shallow depth, in order to be shallower than Northern Lena Trough (Fig. 3 and 9). In terms of SiO_2 and FeO*, the studied Central Lena Trough melts have similar composition to experimental melts at 10 kbar (see Fig. 8). However, such a pressure is strongly unlikely because Central Lena Trough lavas have a strong garnet signature (Fig. 5). Garnet is not stable at 10 kbar in a peridotite assemblage. Central Lena Trough samples have, at a given FeO*, higher Na_2O content. This may reflect a lower degree of partial melting than the experiments. Thus from the comparison to experimental result [26, 27], Central Lena Trough samples may be generated by very low degree partial melting (<5%). However, this comparison is inconsistent for the pressure, due to the garnet signature which requires deep melting, assuminga peridotite assemblage.

Another possibility is a peridotite hydrous melting [30]. This is based on the lack of plagioclase crystallization (see above) and on the high vesicles content. In this frame we compare these samples with experimental results obtain at 10 kbar under hydrous conditions [30] (Fig. 8). In the Na_2O-FeO* diagram, Central Lena Trough Na_2O content is higher, at a given FeO*, than experimental result (Fig. 9). This suggests lower degree partial melting than those experiments [30]. Taking into account that the degree of partial melting given by this experimental work [30] has to be interpreted with caution (see [31]), we estimate nevertheless that the degree partial melting should be lower than 12%. Furthermore, thermodynamic based models [31] show that the degree of partial melting should be lower than those of the Hirose et al experiments [30], at a given water content in the source. Consequently, hydrous, shallow (~10 kbar) and low degree partial melting (F<12%) could generate the major element composition of the Central Lena Trough MORB. This F% estimate might consistent with previous work (F%=7-10) [9]. However, there is still the contradiction with garnet presence at shallow depth in a peridotite assemblage.

4.2.2 Assuming a pyroxenite source

The Central Lena Trough samples are interpreted as having a highly fertile source with a garnet signature (high $(Dy/Yb)_{PM}$ ratio). Furthermore, low degree partial melting [high La/Sm ratio] at shallow pressure (high SiO_2 and low FeO contents) generates these melts. From these source characteristics, a garnet peridotite source is strongly unlikely

because such a source is only stable at great depth (deeper than 60 to 80 km, so 18 to 24 kbar). In contrast, a pyroxenitic source is potentially adequate because it resolves the inconsistency between trace element compositions and major element compositions. Indeed, pyroxenite (i.e pyroxenite source mainly composed by pyroxene) extends the garnet stability field towards shallower pressure (13-17 kbar), which overlaps the spinel-peridotite stability field [32]. Thus, in this assemblage, a garnet phase is stable in the spinel peridotite field. From these characteristics, a pyroxenitic source is a strong likelihood. If a pyroxenite source is involved, there are three possibilities as to its nature: *1)* a garnet eclogite-derived melt (i.e. silica rich pyroxenite), or *2)* Silica poor garnet-pyroxenite-derived melt, *3)* or derived from a peridotite refertilized by garnet-pyroxenite/eclogite-derived melt.

4.2.2.1 Garnet-bearing source

In this case, the Central Lena Trough melts issue from eclogite (clinopyroxene-garnet-coesite) partial melting. As described above, these melts have a major element composition similar to these observed by experimental or numerical studies [18, 32-35]. Eclogite-derived melts are characterized by high silica content [36, 37] and are extremely reactive with the surrounding peridotite. Yaxley et al show that a high-Si liquid is highly reactive with olivine bearing peridotite [36, 37], by dissolving olivine and producing pyroxene. The result of this reaction depends of the amount of Si-rich melt, as we will discuss in the next section. Thus, taking into account the reactivity of eclogite derived melt,

it is unlikely that Central Lena Trough are direct eclogite derived melt.

4.2.2.2 Pyroxenite source: large amount of Si-rich melt.

To produce an olivine-free pyroxenite source[38] by reaction with high Si-melt, a high proportion of eclogite-derived melt is required. The high-Si melt proportion is between 40 to 60 wt% to produce olivine-free pyroxenite [38]. While the eclogite will melt earlier (at higher pressure) because its solidus temperature is substantially lower than the peridotite [39], the amount of eclogite must be relatively large to obtain such a large fraction of high-Si melt. In order to produce a large amount of eclogite in the mantle, the melt productivity under Lena trough would have to be high, and thus a thick basaltic crust would be observed, as in a plume-ridge interaction setting. Moreover, a larger proportion of eclogite in the mantle has geophysical consequences, such as increasing magma flux [38]. In contrast, Lena Trough is considered as an "amagmatic" segment with the slowest effective spreading rate so far on Earth. Consequently, it is unrealistic to consider large amount of eclogite under Lena Trough. In addition, Sobolev et al [38] show that partial melting of pyroxenite produces basalts with a high Ni content melt. Thus, if such a pyroxenite is involved in the Central Lena Trough melts, we should observe a positive correlation between Ni content and $(Dy/Yb)_{PM}$ ratio. In opposite, we observe a negative correlation (not shown), of $(Dy/Yb)_{PM}$ with Ni content ranging from 80 to 134 ppm. In comparison, the northern Lena Trough samples have even higher Ni contents (125 to 166 ppm). However, taking into account the strong influence of S on Ni content [40], the lack

of constraint on S-Ni complex fractionation, the negative correlation between Ni content and $(Dy/Yb)_{PM}$ does not signify necessary that olivine-free pyroxenite is not involved in the Central Lena Trough melt generation. Consequently, we can not use Ni content to rule out a the possibility of an olivine free pyroxenite in the source absolutely.

4.2.2.3 Websterite source: Peridotite metasomatized by Si-rich melt

Here, we look at the situation for a websterite (i.e. olivine-pyroxenite). The difference between a metasomatized peridotite (i.e. enriched in pyroxene relative to a "normal" peridotite) and a websterite is soft. Indeed, this depends on the amount of metasomatic agent. To produce a websterite source (pyroxenite with small amount of olivine) by reaction with high Si-melt, only a small amount (<40 wt%) of eclogite-derived melt is required. In other terms, if the amount of Si-rich melt is not enough to dissolve all olivine then the peridotite is changed into pyroxene enriched peridotite or websterite.

In this context, we compare with experimental results obtained by melting a source composed by a mixture of peridotite and MORB [41]. These experiments produced at low pressure melts with high Al_2O_3 (up to 19.86 wt%), low CaO and FeO (5.79 and 6.37 wt%, respectively) and with Mg# (~0.66-0.67) similar to Central Lena Trough melts (see experiment KG2/KH-39 at 1.5 GPa and 1300ºC, [41]). This scenario might be likely. However, there are still some uncertainties about the pressure and melting degree for Central Lena Trough. In this scenario, the eclogite derived melt is enriched in Dy relative

to Yb, and thus generates a websterite source with high Dy/Yb ratio by reaction with the surrounding peridotite. An equivalent scenario has been proposed to explain the origin of E-MORB [42]. However, it is important to point out the strong differences between the Central Lena Trough basalts and EMORB. Perhaps the most important distinction is in major elements, where the Central Lena Trough basalts have high Al_2O_3 and high SiO_2 – nearly all EMORB have SiO2 less than 50%.

Here, we do not propose trace element model about degree of partial melting, amount of eclogite derived-melt, and so forth for this scenario. Such modeling contains uncertainties on eclogite source composition, amount of melt required to enriched the peridotite, degree of partial melting of eclogite and websterite are so large that it is very easy and not very constraining to reproduce the trace element pattern for Central Lena Trough. A important point here is to notice that garnet phase is not necessary present in the websterite. The high Dy/Yb ratio in melt derives from a high Dy/Yb ratio in the websterite, itself derived from the preferential enrichment in Dy relative to Yb by the (garnet)-eclogite derived melt.

To summarize, we infer that the Central Lena Trough source is a websterite, generated by reaction between a small amount of eclogite derived melt and a peridotite. While weemphasize the presence of websterite in the Central Lena Trough source, we cannot determine the origin of the pre-existing eclogite. However, it might make sense to relate such eclogite to a continental lithospheric component due to the vicinity of continental margins (Greenland and Svalbard) (Fig. 1). Such a continental influence is suggested for the northern segments of the Mid-Atlantic Ridge (MAR) [43], and is born out by the iso-

topic evidence (Nauret et al., in prep).

4.3 Mixing relationships along Lena Trough and westernmost Gakkel Ridge.

While there are clear differences between westernmost Gakkel Ridge,-Northern and Central Lena Trough in terms of major and trace element compositions, they still seem related each other by some kind of mixing relationship. This is illustrated in Fig. 10 with Rb/Nb versus Ba/Nb and Ba/La versus Nb/La and Zr/Y versus Ta/Y. Binary mixing is characterized by hyperbolic relationships which degenerate into straight lines when the denominators of both coordinates are the same [44]. Consequently, in these plots (Fig. 9), westernmost Gakkel Ridge-Northern and Central Lena Trough samples plot on a single line, with R^2 higher than 0.9. Thus, these samples are interpreted as generated by two components mixing. This mixing hypothesis is confirmed also by Nd-Pb-Hf isotopes (Nauret et al., in prep). Furthermore, from the correlation between $(La/Sm)_N$ and $(Dy/Yb)_N$, (Fig. 10), we suggest that the enriched component represented by central Lena Trough samples is preferentially sampled by low degree partial melting (i.e. high La/Sm ratio) and generates a garnet signature (Fig. 9). By contrast, the depleted component is represented by westernmost Gakkel Ridge-Northern Lena Trough samples.

4.4 Consequences for mantle evolution

While westernmost Gakkel Ridge-northern Lena Trough MORB are interpreted as generated by partial melting of spinel lherzolite with some inputs of an enriched com-

ponent. The central Lena Trough is generated or is strongly influenced by highly fertile component having a garnet signature. The Lena Trough mantle is consequently illustrated as a peridotite mantle bearing discrete zones of an enriched component, ie a marble cake [45]. Therefore, we suggest that the amount of eclogite derived melt (and potential the amount of eclogite) decreases from the central part of Lena Trough to the northern part. This can be related to the increase of the distance between the spreading ridge and continental margins (Greenland and Svalbard) or to the increase of the degree of partial melting. If the degree of partial melting increases, then the influence of the spinel-peridotite increases and thus, the signal of the websterite is diluted. This effect is observable in the Lena Trough basalts only because of the depression of the overall degree of partial melting die to the presence of the nearby continents, the slowness of the spreading, and the obliquity of the rift. We suggest that the Lena Trough represents an extreme endmember of the depression of melt productivity.

An important question remains whether the extreme melting beneath Lena Trough is an extreme case of low-degree melting of a normal asthenospheric MORB source, or whether ancient subcontinental lithospheric mantle components are involved in the source. Certainly isotopic investigation now underway (Nauret, et al., in prep) will help to resolve this issue. However, given that we have shown that the Central Lena Basalts are derived from concentrated, discrete heterogeneities, it is not at all clear that these heterogeneities could not survive the process of mantle convection, and they might plausibly have an ancient isotopic signature. This would mean that it is much harder to distinguish between a subcontinental lithospheric source and an asthenospheric source for basalts

than we have assumed until now.

5 CONCLUSIONS

Basalts recovered from the ultra-slow and highly oblique Lena Trough have unique major and trace element compositions, especially for the Central Lena Trough lavas. They are interpreted as being nearly primitive mantle melts, even with low MgO (5.0-6.5 wt%), with no detectable modification by subsequent low-pressure fractionational crystallization. Consequently, Fe and Na values normalized to a constant MgO content appropriate for normal MORB [16, 17] have no meaning in this present situation. We have demonstrated that the source of Central Lena Trough cannot be a peridotite, based on the major and trace element compositions of the basalts generated. We interpret the source as being an olivine websterite generated by reaction between a small amount of an eclogite derived melt and peridotite. This explains the shallow melting and the garnet signature even if a garnet phase is not required to be present within the source and the unique major-trace element composition. We also show that all the melts along Lena Trough and westernmost Gakkel Ridge are influenced by the websterite Lena Trough component, since these melts are generated by the same binary mixing. The chemical variation along Lena Trough and westernmost Gakkel Ridge are consequently related as a decrease of the websterite component related to the variation of the degree of partial melting and/or the increase of the distance between continental margin (Greenland or Svalbard) and the spreading ridge.

Tables and Figures captions

Table 1: Samples locations, Ridge depth, techniques for sample collection, date of EMP and LA-ICP-MS analyses, and number of mineral mounts.

Table 2: Major and trace element compositions. For analytical procedures, see text.

Fig. 1: Bathymetric map and sample locations for Lena Trough. Data are from cruises ARK XX/2, ARK XVII/2 (PFS POLARSTERN, Alfred Wegenr Insitute for Polar and Marine Research) HLY 0102 (USCGC Healy) Each round symbol is a pie chart showing the relative proportions of the lithologies shown in the key. The inset map shows the relationship of the field area to the Greenald and Svalbard margins.

Fig. 2: Na_2O+K_2O versus SiO_2 (wt%). Central Lena Trough samples are reported in solid symbols, Westernmost Gakkel Ridge and Northern Lena Trough samples by open symbols. Database for Pacific, Atlantic and Indian MORB are from PETDB Lamount database (www.petdb.org). While MORB essentially plot in the basalt field, Central Lena Trough and rare Indian MORB samples plot into at the border between trachy-basalt and basaltic trachy-andesite fields.

Fig. 3: Major elements versus MgO (wt%). Samples symbols as in Fig. 2. Except for CaO and K_2O/TiO_2, there are no compositional variations versus MgO for Central Lena Trough (C.L.T.) samples. Westernmost Gakkel Ridge (W.M.G.R.) and Northern Lena Trough (N.L.T.) samples display limited range of chemical variation. In all diagrams, samples 219-2 plot between Central and Westernmost Gakkel Ridge-Northern Lena

Trough fields. For comparison, we report MAR MORB (gray dot) from PETDB Lamount database (www.petdb.org), experiment for low degree partial melting of peridotite [26, 27], partial melting of peridotite (1 to 3 GPa) [23, 24], and KG2 pyroxenite partial melting [41]

Fig. 4: $Na_{8.0}$ versus $Fe_{8.0}$ diagram modified after [46] and incorporated Gakkel MORB values from [10]. Central Lena Trough melts plots at an extremity of the correlation, with low $Fe_{8.0}$ and high $Na_{8.0}$.

Fig. 5: Trace element diagrams, normalized to primitive mantle [20]. Red lines correspond to Central Lena Trough samples, blue lines for Westernmost Gakkel Ridge-Northern Lena Trough. With depleted HREE relative to MREE, Central Lena Trough display a clear garnet signature. While westernmost Gakkel Ridge and Northern Lena Trough samples display higher concentration than N-MORB [20], they have similar pattern than N-MORB (MgO 8 wt%) (open dot), reflecting shallow crystallisation fractionation.

Fig. 6: Liquid line descent (LLD) calculation for shallow pressure crystallization (0.5 Kbar) done with MELT [21]. For Central Lena Trough, LLD are calculated for 0 and 0.5 wt% H_2O. With these calculations, we demonstrate that CLT major element variations cannot be explained by shallow pressure crystallization of plagioclase, olivine and cpx. For Northern Lena Trough and Westernmost Gakkel Ridge, calculations are done with 0 wt% H_2O. Northern Lena Trough and Westernmost Gakkel Ridge basalts fall general-

lyon liquid lines descent. Also, we show that CLT cannot derived from shallow pressure crystallization of Northern Lena Trough and Westernmost Gakkel Ridge liquids. Same symbols as in Fig. 2.

Fig. 7: Test for olivine, plagioclase and clinopyroxene fractionation. Same symbols as in Fig. 2. A) Y versus MgO. Central Lena Trough samples displays constant Y content for MgO ranging from 5 to 6.5 wt%, suggesting any olivine fractionation. Based on limited variations of Y content for Westernmost Gakkel Ridge-Northern Lena Trough, we cannot decipher if these samples are affected by Olivine fractionation, although such process is supposed. B) Sc versus MgO. Due to the Sc compatibility in Clinopyroxene (Cpx), a decrease of Sc may reflect Cpx fractionation. Based on constant Sc concentrations for Central and Lena Trough samples, no clear Cpx fractionation is observed. C) Eu/Eu* versus MgO. Eu/Eu* is used as a tracer for plagioclase fractionation. Eu/Eu* upper than 1 may reflect plagioclase accumulation or source characteristic whereas Eu/Eu* lower than 1 reflects plagioclase fractionation. There is no correlation between Eu/Eu* versus MgO for Central and Westernmost Gakkel Ridge-Northern Lena Trough samples. Central Lena Trough and 291-2 samples display Eu/Eu* higher than 1. Westernmost Gakkel Ridge and Northern Lena Trough samples have Eu/Eu* lower than 1. D) Eu/Eu* versus (Sr/Nd) ratio normalized to primitive mantle [20]. Both ratios are used as plagioclase fractionation tracer. There is no correlation between Eu/Eu* and $(Sr/Nd)_{PM}$. This suggests that Central and Westernmost Gakkel Ridge-Northern Lena Trough, and 219-2 samples are not affected by shallow plagioclase fractionation. Thus, Central Lena Trough and 219-2

samples have mantle source characterized by high Eu/Eu* and $(Sr/Nd)_{PM}$

Fig. 8: $(La/Sm)_{PM}$ versus $(Dy/Yb)_{PM}$. (La/Sm) ratio is used a degree of partial melting trace. High La/Sm ratio is for low degree of partial melting and low La/Sm ratio is for high degree partial melting. (Dy/Yb) ratio is used as a garnet tracer. High (Dy/Yb) ratio illustrates garnet bearing source. We observe that Central Lena Trough samples have higher $(La/Sm)_{PM}$ and $(Dy/Yb)_{PM}$ ratio than Westernmost Gakkel Ridge-Northern Lena Trough. That suggests that Central Lena Trough are affected by lower degree of partial melting with residual garnet in the mantle, compare to Westernmost Gakkel Ridge and Northern Lena Trough. Again, 219-2 samples plot between Central and Westernmost Gakkel Ridge-Northern Lena trough samples. We also observe a positive correlation between $(La/Sm)_{PM}$ and $(Dy/Yb)_{PM}$ for Central Lena Trough samples. This suggests that the garnet signature disappears when degree of partial melting increases. In comparison with literature data from EPR, MAR and Indian ridges (PETDB Lamount database: www.petdb.org) (same symbols as in Fig. 2), westernmost Gakkel Ridge-northern Lena trough melts have similar composition to other MORB.

Fig. 9: Comparison between experimental major element composition and studied samples. A) SiO_2 versus FeO_{total}. SiO_2 and FeO_t are used a tracer for pressure of melting. To illustrate the FeO-SiO_2 dependence to the pressure, we report melt compositions generated by peridotite partial melting (Per. Melt) between 1 and 3 GPa [23, 24]. Westernmost Gakkel Ridge and Northern Lena Trough (WMGR-NLT) compositions plot between 10-20 kbar experimental melt compositions. Central Lena Trough (CLT) compositions are

compared first with experimental melts produced at 1 GPa in anhydrous condition with low degree partial melting [27-29, 47]. Second, Central Lena Trough melts are compared to hydrous partial melts (Hy. Per. Melt) also generated at shallow pressure (1 GPa) (experiements done a T=1100 °C and at T=1200 °C) [30]. Third, Central Lena Trough melts are compared with eclogite derived melt (Eclo. Melt) generated at 3 GPa [35]. Based on similarities between 1 GPa experimental melts and studied compositions, we interpret Central Lena Trough melt as being generated at ~1 GPa. B) Na_2O versus FeO_t. Na_2O is used as trace for degree of partial melting. We compare Central and Northern Lena Trough composition to same experiments than in Fig. 8-a. In this diagram, Northern Lena Trough Na_2O contents suggest a degree of partial melting between 29 and 30% at 1 GPa or between 12 and 28% at 2 GPa. Due to major and trace element compositions of Westernmost Gakkel Ridge-Northern Lena Trough MORB, we consider that these melt were produced by 12-20% of partial melting, as classically interpreted for N-MORB [16, 17]. With high Na_2O contents (~4 wt%), Central Lena Trough samples are interpreted as being generated in hydrous conditions with less than 12% of partial melting (detail: see text).

Fig. 10: Rb/Nb versus Ba/Nb, Ba/La versus Nb/La and Ta/Y versus Zr/Y. In each diagram, ratios share common denominator. Consequently, a potential binary mixing hyperbola degenerates to a line [44]. In each diagrams, a linear relationship with a good coefficient correlation (r^2 higher than 0.97) is observed. This coefficient r^2 is simply calculated using Excel. As a consequence, Central and Northern Lena Trough and westernmost Gakkel Ridge are related and generated by a binary mixing relationship.

Central Lena Trough											
Cruise	Comment	Lon	Lat	Depth	Ridge-Depth	Method	Mount	EMP Date	N	LA-Date	N
PS-66	262-92	-2.507	80.907	3545	3545	Dredge	FN 3	Jan-05	-1	Jan-05	3
PS-66	262-83	-2.507	80.907	3545	3545	Dredge	FN 3	Jan-05	-1	Jan-05	3
PS-66	262-35	-2.507	80.907	3545	3545	Dredge	FN 3	Jan-05	-1	Jan-05	3
PS-66	262-34	-2.507	80.907	3545	3545	Dredge	FN 3	Jan-05	-1	Jan-05	3
PS-66	262-21	-2.507	80.907	3545	3545	Dredge	FN 3	Jan-05	-1	Jan-05	3
PS-66	261-71	-2.525	80.924	3570	3570	Dredge	FN 3	Jan-05	-1	Jan-05	3
PS-66	261-5	-2.525	80.924	3570	3570	Dredge	FN 3	Jan-05	-1	Jan-05	3
PS-66	261-47	-2.525	80.924	3570	3570	Dredge	FN 3	Jan-05	-1	Jan-05	3
PS-66	261-1	-2.525	80.924	3570	3570	Dredge	FN 3	Jan-05	-1	Jan-05	3
PS-66	261-17	-2.525	80.924	3570	3570	Dredge	FN 3	Jan-05	-1	Jan-05	3
PS-66	261-12	-2.525	80.924	3570	3570	Dredge	FN 3	Jan-05	-1	Jan-05	3
PS-55	90-1	-2.508	80.908	3550	3550	Dredge	FN1	13-May-06	4	Jan-05	3
PS-55	90-3	-2.508	80.908	3550	3550	Dredge	FN1	13-May-06	5	Jan-05	3
PS-55	90-4	-2.508	80.908	3550	3550	Dredge	FN1	13-May-06	4	Jan-05	3
PS-55	90-7	-2.508	80.908	3550	3550	Dredge	FN1	13-May-06	5	Jan-05	3
PS-55	90-10	-2.508	80.908	3550	3550	Dredge	FN1	13-May-06	4	Jan-05	3
PS-55	90-27	-2.508	80.908	3550	3550	Dredge	FN1	13-May-06	4	Jan-05	3
Northern Lena Trough											
PS-66	219-2	-6.541	82.785	4890	4950	Dredge	FN 2	Jan-05	-1	Jan-05	3
PS-66	219-1	-6.541	82.785	4890	4950	Dredge	FN 2	Jan-05	-1	Jan-05	3
PS-66	217-9	-6.147	82.857	4792	4800	Dredge	FN 2	Jan-05	-1	Jan-05	3
PS-66	217-8	-6.147	82.857	4792	4850	Dredge	FN 2	Jan-05	-1	Jan-05	3
PS-66	217-7	-6.147	82.857	4792	4850	Dredge	FN 2	Jan-05	-1	Jan-05	3
PS-66	217-6	-6.147	82.857	4792	4850	Dredge	FN 2	Jan-05	-1	Jan-05	3
PS-66	217-4	-6.147	82.857	4792	4850	Dredge	FN 2	Jan-05	-1	Jan-05	3
PS-66	217-3	-6.147	82.857	4792	4850	Dredge	FN 2	Jan-05	-1	Jan-05	3
PS-66	217-1	-6.147	82.857	4792	4850	Dredge	FN 2	Jan-05	-1	Jan-05	3
HLY-0102	D8-16	-6.260	82.890	3982	4225	Dredge	G 7	18-Jul-05	6	10/02/2005	4
HLY-0102	D8-11	-6.260	82.890	3982	4225	Dredge	T 1	20-Jul-05	4	17/03/2005	4
HLY-0102	D8-13	-6.260	82.890	3982	4225	Dredge	T 1	20-Jul-05	4	17/03/2005	4
HLY-0102	D8-16	-6.260	82.890	3982	4225	Dredge	T 1	20-Jul-05	5	17/03/2005	6
HLY-0102	D8-17	-6.260	82.890	3982	4225	Dredge	T 1	20-Jul-05	3	17/03/2005	6
HLY-0102	D8-1	-6.260	82.890	3982	4225	Dredge	T 1	20-Jul-05	3	17/03/2005	6
HLY-0102	D8-21	-6.260	82.890	3982	4225	Dredge	T 1	20-Jul-05	4	17/03/2005	6
HLY-0102	D8-22	-6.260	82.890	3982	4225	Dredge	T 1	20-Jul-05	3	17/03/2005	6
HLY-0102	D8-8	-6.260	82.890	3982	4225	Dredge	T 1	20-Jul-05	4	17/03/2005	4
HLY-0102	D11-19	-6.320	83.000	3987	4105	Dredge	T 2	20-Jul-05	3	17/03/2005	4
HLY-0102	D11-22	-6.320	83.000	3987	4105	Dredge	T 2	20-Jul-05	3	17/03/2005	5
HLY-0102	D11-5	-6.320	83.000	3987	4105	Dredge	T 2	20-Jul-05	4	17/03/2005	4
HLY-0102	D11-9	-6.320	83.000	3987	4105	Dredge	T 2	20-Jul-05	4	17/03/2005	4
Westermost Gakkel Ridge											
PS-66	214-7	-4.924	82.973	2269	4400	Dredge	FN 2	Jan-05	-1	Jan-05	3
PS-66	214-5	-4.924	82.973	2269	4400	Dredge	FN 2	Jan-05	-1	Jan-05	3
PS-66	214-3	-4.924	82.973	2269	4400	Dredge	FN 2	Jan-05	-1	Jan-05	3

PS-66	214-2	-4.924	82.973	2269	4400	Dredge	FN 2	Jan-05	-1	Jan-05	3
PS-59	216-SG	-6.040	83.070	3605	3605	TVG	T 3	20-Jul-05	4	18/03/2005	4
PS-59	218-36	-5.750	83.080	3866	4015	Dredge	T 3	20-Jul-05	4	18/03/2005	4
PS-59	218-SG	-5.750	83.080	3866	4015	Dredge	T 3	20-Jul-05	4	18/03/2005	4
PS-59	221-1	-5.578	83.260	4175	4500	TVG	T 3	20-Jul-05	4	18/03/2005	4
PS-59	221-SG	-5.578	83.260	4175	4500	TVG	T 3	20-Jul-05	4	18/03/2005	4
PS-59	223-8	-4.398	83.300	3073	3975	Dredge	T 4	20-Jul-05	4	13/05/2005	8

Table 1.

Comment	262-92	262-83	262-35	262-34	262-21	261-71	261-5	261-47	261-1	261-17	261-12
latitude	80.90	80.90	80.90	80.90	80.90	80.92	80.92	80.9243	80.9243	80.9243	80.9243
longitude	-2.50	-2.50	-2.50	-2.50	-2.50	-2.52	-2.52	-2.5253	-2.5253	-2.5253	-2.5253
SiO_2	51.3	51.1	51.3	51.4	51.2	51.3	51.4	51.1	51.2	51.6	51.5
TiO_2	1.69	1.68	2.21	2.22	1.68	1.59	1.56	1.59	1.55	1.60	1.58
Al_2O_3	18.34	18.33	18.16	18.31	18.44	18.21	18.25	18.10	18.18	18.29	18.15
CaO	9.60	9.52	8.63	8.68	9.56	9.76	9.74	9.69	9.72	9.84	9.72
FeO	6.54	6.52	6.69	6.79	6.57	6.55	6.60	6.55	6.66	6.52	6.63
MgO	6.14	6.10	5.22	5.05	6.14	6.35	6.39	6.48	6.44	6.24	6.46
MnO	0.11	0.15	0.15	0.15	0.12	0.12	0.13	0.13	0.12	0.13	0.13
Na_2O	4.13	4.04	4.00	4.06	4.10	4.20	4.12	4.14	4.11	4.15	4.10
K_2O	1.25	1.26	1.94	1.98	1.24	1.01	1.01	1.01	1.01	1.003	1.008
P_2O_5	0.21	0.20	0.28	0.28	0.22	0.20	0.20	0.19	0.17	0.184	0.183
S	0.05	0.05	0.04	0.05	0.06	0.05	0.06	0.04	0.06	0.05	0.06
Cl	0.02	0.02	0.04	0.03	0.02	0.02	0.02	0.02	0.02	0.02	0.02
Total	99.41	98.94	98.69	99.01	99.31	99.37	99.41	99.02	99.26	99.62	99.49
Cs	0.613	0.625	1.057	1.032	0.605	0.488	0.483	0.489	0.484	0.475	0.475
Rb	44.71	46.42	74.29	73.17	44.84	36.75	37.31	36.70	36.35	36.06	35.89
Ba	416	420	682	679	417	352	346	356	337	345	335
Th	1.172	1.088	1.773	1.813	1.083	0.962	0.911	0.960	0.894	0.938	0.889
U	0.344	0.347	0.561	0.585	0.349	0.298	0.285	0.298	0.284	0.295	0.277
Nb	24.06	24.78	39.90	40.18	24.67	21.64	20.91	21.36	21.15	21.20	20.29
Ta	1.681	1.709	2.683	2.784	1.730	1.473	1.426	1.484	1.403	1.432	1.380
La	12.68	12.81	18.60	18.63	12.71	11.69	11.37	11.77	11.04	11.48	10.95
Ce	31.56	32.35	45.16	45.38	32.04	29.87	28.91	30.08	28.52	29.23	28.06
Sr	495	496	622	621	495	450	454	445	453	445	444
Pb	1.463	1.519	1.948	1.948	1.468	1.445	1.387	1.442	1.375	1.443	1.349
Nd	20.92	21.34	28.49	28.86	21.06	20.08	19.45	20.27	19.45	19.54	18.91
Zr	188	191	246	254	194	183	173	177	175	178	171
Hf	4.395	4.494	5.636	5.940	4.554	4.357	4.133	4.255	4.082	4.251	4.030
Sm	5.137	5.248	6.593	6.694	5.172	5.106	4.937	5.153	4.869	4.954	4.819
Eu	1.907	1.911	2.356	2.347	1.880	1.879	1.831	1.916	1.823	1.827	1.795
Gd	5.551	5.727	6.696	6.821	5.648	5.853	5.623	5.777	5.541	5.673	5.491
Tb	0.871	0.894	0.993	1.005	0.888	0.935	0.884	0.938	0.889	0.901	0.878
Dy	5.276	5.377	5.801	5.914	5.395	5.827	5.509	5.798	5.539	5.640	5.347
Ho	1.035	1.059	1.110	1.140	1.069	1.167	1.100	1.164	1.102	1.142	1.071
Er	3.015	3.075	3.125	3.200	3.059	3.415	3.186	3.380	3.179	3.280	3.074
Tm	0.410	0.416	0.415	0.433	0.418	0.463	0.429	0.462	0.432	0.453	0.425
Y	29.31	30.06	30.90	31.97	30.32	32.91	30.53	31.80	30.82	32.18	30.49
Yb	2.760	2.801	2.864	2.851	2.829	3.144	2.954	3.103	2.936	3.054	2.823
Lu	0.404	0.409	0.413	0.424	0.416	0.460	0.433	0.445	0.423	0.448	0.415
Ni	109	113	79	79	113	124	130	132	129	122	125
Sc	41.17	40.88	37.85	39.37	41.88	43.51	43.09	41.80	43.05	43.90	43.03

Table 2

	1	3	4	7	9	10	27
	Central Lena Trough (ARK XV/2)						
latitude	80.908	80.908	80.908	80.908	80.908	80.908	80.908
longitude	-2.508	-2.508	-2.508	-2.508	-2.508	-2.508	-2.508
SiO_2	51.5	51.4	51.5	51.6	51.8	51.5	51.4
TiO_2	2.00	2.00	2.01	2.02	2.02	2.03	2.01
Al_2O_3	18.30	18.31	18.35	18.36	18.36	18.34	18.32
CaO	9.01	9.00	9.10	8.97	9.10	8.94	8.99
FeO	6.64	6.71	6.65	6.59	6.70	6.63	6.67
MgO	5.70	5.71	5.73	5.66	5.62	5.68	5.69
MnO	0.12	0.15	0.13	0.13	0.13	0.13	0.14
Na_2O	3.87	3.84	3.88	3.95	3.89	3.90	3.89
K_2O	1.54	1.55	1.55	1.56	1.51	1.55	1.55
P_2O_5	0.27	0.27	0.26	0.27	0.28	0.26	0.27
S	0.05	0.04	0.04	0.04	0.05	0.04	0.05
Cl	0.02	0.03	0.03	0.03	0.03	0.03	0.03
Total	99.015	99.032	99.180	99.140	99.439	98.994	99.003
Cs	0.828	0.841	0.823	0.83	0.500	0.816	0.849
Rb	59.7	60.07	58.82	60.83	38.06	59.35	60.20
Ba	552	551	541	550	346	545	553
Th	1.465	1.446	1.578	1.427	0.923	1.413	1.433
U	0.465	0.454	0.447	0.453	0.280	0.458	0.466
Nb	32.32	32.509	31.384	32.059	19.297	31.818	32.147
Ta	2.281	2.263	2.227	2.25	1.350	2.226	2.268
La	16.009	15.971	15.775	15.815	9.999	15.658	15.871
Ce	39.80	39.66	39.23	39.59	25.16	39.22	39.99
Sr	575	571	562	565	374	564	569
Pb	1.836	1.878	1.786	1.756	1.087	1.813	1.86
Nd	26.21	25.84	25.60	25.72	15.96	25.36	25.87
Zr	237	237	232	232	145	229.6	232
Hf	5.591	5.505	5.442	5.426	3.375	5.424	5.458
Sm	6.276	6.125	6.143	6.115	3.952	6.055	6.1
Eu	2.244	2.19	2.195	2.203	1.396	2.187	2.218
Gd	6.608	6.527	6.514	6.482	3.946	6.35	6.458
Tb	1.008	0.993	0.992	0.981	0.614	0.971	0.987
Dy	6.037	5.894	5.955	5.914	3.585	5.803	5.856
Ho	1.181	1.16	1.147	1.153	0.706	1.142	1.146
Er	3.37	3.29	3.291	3.294	1.907	3.227	3.251
Tm	0.459	0.445	0.455	0.446	0.289	0.439	0.446
Y	32.99	32.84	32.31	32.12	19.41	31.84	32.07
Yb	3.05	2.999	3.013	3.015	1.834	3.007	2.972
Lu	0.458	0.445	0.439	0.437	0.264	0.429	0.438
Ni	98	97	95	96	85	93	97
Sc	41.53	41.21	41.13	40.35	24.24	40.36	41.05

Table 2 (continued)

	217-5	217-6	217-7	217-4	217-8	217-9	217-1	217-3	219-1	219-2	VG2	ATHO
latitude	82.85	82.85	82.85	82.85	82.85	82.85	82.85	82.85	82.78	82.78		
longitude	-6.14	-6.14	-6.14	-6.14	-6.14	-6.14	-6.14	-6.14	-6.54	-6.54		
SiO_2	52.2	50.6	50.5	50.7	50.6	50.7	50.6	50.4	50.5	49.4	50.9	
TiO_2	1.79	1.75	1.74	1.76	1.72	1.78	1.74	1.75	1.77	1.91	1.89	
Al_2O_3	16.39	16.01	15.79	15.97	15.84	15.96	16.07	15.97	15.95	17.45	14.06	
CaO	10.99	10.66	10.64	10.67	10.65	10.75	10.65	10.65	10.63	10.29	11.02	
FeO	10.02	9.62	9.70	9.60	9.72	9.65	9.53	9.55	9.65	9.76	11.88	
MgO	7.33	7.12	7.11	7.14	7.50	6.88	7.06	7.11	7.23	6.63	6.72	
MnO	0.170	0.187	0.158	0.158	0.195	0.168	0.178	0.157	0.178	0.165	0.21	
Na_2O	1.44	3.40	3.32	3.38	3.38	3.42	3.39	3.35	3.32	3.54	2.89	
K_2O	0.350	0.363	0.364	0.365	0.366	0.367	0.367	0.369	0.359	0.663	0.19	
P_2O_5	0.159	0.174	0.161	0.159	0.164	0.153	0.166	0.168	0.159	0.121	0.22	
S	0.11	0.10	0.10	0.10	0.10	0.11	0.11	0.10	0.12	0.09	0.13	
Cl	0.01	0.01	0.01	0.01	0.01	0.01	0.01	0.01	0.01	0.01	0.03	
Total	100.95	100.05	99.60	99.99	100.28	99.95	99.90	99.56	99.90	100.04		
Cs	0.150	0.169	0.165	0.169	0.173	0.163	0.167	0.153	0.164	0.453		0.860±0.018
Rb	10.81	11.30	11.30	11.17	11.43	11.23	11.77	11.68	11.66	24.69		59.61±1.0
Ba	111	116	120	114	119	118	115	121	115	225		534±7
Th	8.430	0.665	0.501	0.524	0.488	0.489	0.500	0.492	0.482	0.954		7.287±0.129
U	0.135	0.144	0.141	0.135	0.142	0.143	0.142	0.140	0.138	0.240		2.238±0.039
Nb	6.81	7.43	7.75	7.25	7.66	7.59	7.32	7.73	7.70	11.67		58.0±0.6
Ta	0.380	0.487	0.512	0.490	0.509	0.495	0.495	0.512	0.515	0.824		3.589±0.067
La	6.352	6.774	7.080	6.803	6.980	7.098	6.650	7.067	6.711	8.282		53.4±0.6
Ce	17.59	19.75	20.62	19.77	20.43	20.80	18.89	20.77	19.74	22.74		118±1
Sr	247	265	270	257	266	268	253	267	266	380		96±1
Pb	1.817	0.856	0.872	0.869	0.875	0.880	0.826	0.892	0.918	1.593		5.655±0.492
Nd	15.56	17.48	18.03	17.53	17.90	18.32	17.00	18.20	17.29	17.68		58±1
Zr	151	162	171	159	167	172	149	169	165	141		503±9
Hf	3.973	4.256	4.532	4.269	4.471	4.600	3.973	4.560	4.458	3.852		13.54±0.31
Sm	5.530	5.698	5.768	5.571	5.816	5.940	5.497	5.855	5.547	5.075		13.4±0.2
Eu	1.798	2.077	2.131	2.078	2.146	2.172	1.997	2.144	2.050	1.986		2.63±0.04
Gd	6.516	7.559	7.860	7.529	7.795	7.973	7.155	7.885	7.497	6.213		14.77±0.21
Tb	1.123	1.309	1.357	1.296	1.339	1.376	1.255	1.364	1.295	1.033		2.502±0.037
Dy	7.552	8.434	8.847	8.448	8.752	8.997	8.012	8.861	8.535	6.487		16.04±0.23
Ho	1.636	1.766	1.850	1.738	1.831	1.873	1.668	1.849	1.767	1.320		3.329±0.058
Er	4.749	5.202	5.407	5.249	5.466	5.536	4.736	5.435	5.222	3.808		10.09±0.18
Tm	0.662	0.718	0.745	0.724	0.752	0.769	0.688	0.746	0.724	0.518		1.459±0.025
Y	43.45	49.68	52.13	48.66	50.68	52.60	44.92	51.07	49.84	37.75		96±2
Yb	4.397	4.928	5.094	5.016	5.054	5.245	4.816	5.125	5.066	3.533		10.16±0.14
Lu	0.633	0.721	0.763	0.711	0.756	0.770	0.683	0.754	0.740	0.516		1.504±0.031
Ni	117	142	148	139	167	154	130	151	158	127		3.958±1.018
Sc	51.89	54.07	56.59	53.35	56.09	57.53	51.10	56.30	56.53	50.08		5.976±0.146

Table 2 (continued)

Cruise	HLY-0102	HLY-0102	HLY-0102	HLY-0102	HLY-0102	HLY-0102	HLY-0102	HLY-0102	HLY-0102	HLY-0102	HLY-0102	HLY-0102
Comment	D8-16	D8-11	D8-13	D8-16	D8-17	D8-1	D8-21	D8-22	D8-8	D11-5	D11-9	D11-22
Lon	-6.26	-6.26	-6.26	-6.26	-6.26	-6.26	-6.26	-6.26	-6.26	-6.32	-6.32	-6.32
Lat	82.89	82.89	82.89	82.89	82.89	82.89	82.89	82.89	82.89	83	83	83
SiO_2	50.7	50.4	50.8	50.7	49.7	50.6	50.8	50.6	50.7	51.0	50.8	50.6
TiO_2	1.50	1.58	1.50	1.52	1.20	1.51	1.55	1.51	1.57	1.56	1.55	1.57
Al_2O_3	15.65	15.42	15.69	15.70	16.66	15.66	15.55	15.67	15.44	16.03	16.06	15.91
FeO	9.33	9.52	9.40	9.34	8.94	9.42	9.51	9.41	9.48	9.24	9.12	9.18
MnO	0.18	0.18	0.17	0.17	0.17	0.16	0.16	0.16	0.17	0.16	0.16	0.16
MgO	7.66	7.61	7.80	7.74	8.24	7.73	7.60	7.73	7.57	7.48	7.47	7.46
CaO	11.03	10.97	10.97	10.94	11.85	10.98	10.95	11.00	11.00	10.88	10.86	10.86
Na_2O	3.17	3.18	3.01	3.18	2.94	3.19	3.14	3.20	3.17	3.14	3.23	3.26
K_2O	0.20	0.21	0.20	0.22	0.07	0.20	0.20	0.20	0.21	0.32	0.31	0.32
P_2O_5	0.15	0.15	0.14	0.13	0.08	0.16	0.14	0.17	0.15	0.16	0.15	0.15
S	0.10	0.11	0.10	0.10	0.11	0.10	0.10	0.11	0.11	0.11	0.10	0.10
Cl	0.01	0.01	0.01	0.01	0.01	0.01	0.01	0.01	0.01	0.01	0.01	0.01
Total	99.73	99.33	99.74	99.75	99.94	99.71	99.70	99.80	99.58	100.11	99.77	99.60
Cs	0.052	0.046	0.049	0.050	0.011	0.048	0.049	0.050	0.047	0.094	0.096	0.091
Rb	3.84	3.52	3.71	3.70	0.62	3.70	3.51	3.72	3.53	6.89	6.85	6.80
Ba	46.9	43.4	44.9	45.7	7.6	44.7	43.8	45.4	43.4	73.6	72.2	71.9
Th	0.247	0.261	0.251	0.238	0.065	0.247	0.253	0.250	0.264	0.301	0.301	0.305
U	0.067	0.067	0.065	0.064	0.021	0.064	0.066	0.065	0.067	0.085	0.085	0.085
Nb	3.22	3.01	3.08	3.17	0.84	3.09	3.09	3.14	3.06	4.99	4.90	4.86
Ta	0.201	0.201	0.208	0.197	0.056	0.205	0.198	0.205	0.202	0.333	0.339	0.339
La	3.84	3.94	3.77	3.76	1.93	3.74	3.93	3.82	3.94	4.49	4.41	4.44
Ce	11.5	11.5	11.0	11.1	6.7	11.0	11.6	11.1	11.5	12.7	12.5	12.4
Sr	154	147	147	150	126	148	147	149	148	175	173	172
Pb	0.535	0.537	0.527	0.543	0.322	0.527	0.548	0.524	0.548	0.553	0.565	0.563
Nd	10.7	11.0	10.6	10.5	7.4	10.5	11.0	10.7	11.1	11.2	11.0	11.1
Zr	98.8	102.6	96.3	94.3	67.7	97.0	100.4	99.2	104.1	99.5	98.7	102.5
Hf	2.60	2.79	2.63	2.46	1.82	2.63	2.68	2.68	2.85	2.57	2.61	2.72
Sm	3.60	3.76	3.58	3.52	2.69	3.53	3.71	3.60	3.77	3.57	3.56	3.57
Eu	1.32	1.35	1.31	1.30	1.08	1.30	1.34	1.31	1.36	1.34	1.32	1.32
Gd	4.81	5.07	4.83	4.60	3.72	4.77	4.94	4.90	5.13	4.62	4.59	4.71
Tb	0.834	0.885	0.836	0.800	0.662	0.833	0.857	0.855	0.897	0.789	0.799	0.806
Dy	5.66	5.98	5.67	5.38	4.51	5.65	5.79	5.79	6.06	5.33	5.28	5.39
Ho	1.18	1.25	1.19	1.12	0.95	1.19	1.21	1.22	1.27	1.10	1.10	1.13
Er	3.45	3.66	3.47	3.26	2.79	3.46	3.54	3.55	3.73	3.21	3.19	3.29
Tm	0.489	0.526	0.494	0.461	0.396	0.493	0.508	0.512	0.530	0.450	0.453	0.468
Y	32.3	33.7	31.6	30.6	25.6	31.9	32.6	32.6	34.2	29.4	29.0	30.4
Yb	3.33	3.51	3.37	3.16	2.73	3.33	3.42	3.40	3.56	3.11	3.11	3.19
Lu	0.488	0.528	0.494	0.464	0.399	0.493	0.505	0.506	0.533	0.449	0.454	0.475
Ni	113	106	112	113	123	111	107	114	109	105	102	111
Sc	40.7	41.8	40.4	39.2	38.4	40.7	40.7	41.1	42.4	38.8	38.6	39.8

Table 2 (continued)

Cruise	PS-59	PS-59	PS-59	PS-59	PS-59	PS-59	PS-66	PS-66	PS-66	PS-66	PS-66
Comment	216-SG	218-36	218-SG	221-1	221-SG	223-8	214-2	214-7	214-5	214-3	214-1
Lon	-6.04	-5.75	-5.75	-5.578	-5.578	-4.398	-4.92	-4.92	-4.92	-4.92	-4.92
Lat	83.07	83.08	83.08	83.26	83.26	83.3	82.97	82.97	82.97	82.97	82.97
SiO_2	50.4	50.9	50.9	50.9	50.7	50.8	50.2	50.2	50.3	50.4	51.6
TiO_2	1.54	1.57	1.56	1.55	1.74	1.50	1.67	1.65	1.64	1.81	1.71
Al_2O_3	15.89	16.26	16.28	16.19	15.82	16.18	16.00	16.04	16.00	15.85	16.45
FeO	9.44	9.01	8.99	8.96	9.62	9.18	11.34	11.22	11.32	10.88	11.74
MnO	0.17	0.16	0.17	0.16	0.17	0.16	9.77	9.78	9.83	10.32	10.22
MgO	7.45	6.92	7.11	7.20	6.94	7.81	7.30	7.36	7.37	7.11	7.37
CaO	11.26	10.87	10.82	10.85	10.95	10.99	0.17	0.19	0.17	0.19	0.17
Na_2O	3.21	3.52	3.53	3.50	3.32	3.13	3.22	3.25	3.26	3.33	1.70
K_2O	0.17	0.25	0.24	0.23	0.21	0.22	0.16	0.17	0.17	0.18	0.15
P_2O_5	0.15	0.17	0.16	0.17	0.17	0.14	0.14	0.16	0.15	0.18	0.15
S	0.10	0.10	0.10	0.10	0.11	0.09	0.10	0.11	0.11	0.12	0.11
Cl	0.01	0.01	0.01	0.01	0.01	0.01	0.00	0.00	0.00	0.00	0.01
Total	99.74	99.71	99.84	99.86	99.73	100.17	100.03	100.14	100.30	100.34	101.39
Cs	0.030	0.055	0.056	0.056	0.043	0.034	0.039	0.042	0.040	0.035	0.042
Rb	2.39	4.32	4.40	4.35	3.22	3.36	3.14	3.10	3.16	2.94	3.28
Ba	30.4	52.3	52.0	51.0	43.0	48.4	37.3	35.5	36.3	34.4	39.1
Th	0.226	0.325	0.325	0.321	0.303	0.374	0.298	0.295	0.292	0.287	0.312
U	0.062	0.083	0.084	0.084	0.082	0.081	0.096	0.091	0.091	0.097	0.096
Nb	2.74	4.04	4.04	3.96	3.64	3.91	3.95	3.76	3.87	4.15	4.12
Ta	0.174	0.261	0.270	0.267	0.221	0.270	0.243	0.236	0.243	0.260	0.259
La	3.78	4.83	4.80	4.72	4.97	4.73	5.781	5.510	5.615	6.369	6.020
Ce	11.3	13.6	13.5	13.4	14.4	11.7	17.92	16.92	17.36	19.80	18.73
Sr	152	178	173	172	169	170	234	230	235	248	242
Pb	0.499	0.610	0.634	0.643	0.599	0.568	0.767	0.757	0.755	0.821	0.812
Nd	10.7	11.8	11.7	11.7	12.8	10.9	16.52	15.50	15.93	17.82	17.23
Zr	101.1	105.7	103.9	102.5	121.0	96.8	160	155	158	182	166
Hf	2.66	2.71	2.67	2.70	2.98	2.58	4.283	4.155	4.128	4.606	4.379
Sm	3.60	3.69	3.68	3.66	4.11	3.55	5.575	5.253	5.353	5.866	5.752
Eu	1.32	1.32	1.33	1.31	1.45	1.28	2.066	1.941	1.963	2.139	2.153
Gd	4.78	4.66	4.63	4.69	5.30	4.78	7.625	7.161	7.331	7.972	7.808
Tb	0.836	0.801	0.800	0.801	0.913	0.822	1.327	1.262	1.291	1.386	1.384
Dy	5.62	5.33	5.31	5.35	6.08	5.50	8.729	8.270	8.406	9.048	9.008
Ho	1.18	1.10	1.09	1.12	1.25	1.15	1.833	1.757	1.771	1.898	1.881
Er	3.42	3.19	3.19	3.19	3.63	3.30	5.373	5.195	5.219	5.585	5.595
Tm	0.489	0.451	0.449	0.459	0.516	0.469	0.742	0.722	0.724	0.779	0.770
Y	32.5	31.0	30.3	30.2	36.0	30.7	51.06	49.72	50.58	54.61	52.91
Yb	3.38	3.13	3.10	3.12	3.59	3.15	5.155	4.942	4.942	5.333	5.240
Lu	0.501	0.467	0.460	0.461	0.527	0.466	0.751	0.732	0.731	0.790	0.780
Ni	99	82	88	94	76	108	158	155	158	144	155
Sc	41.0	37.7	37.9	38.3	41.7	39.4	57.53	57.35	57.43	58.14	59.60

Table 2 (continued)

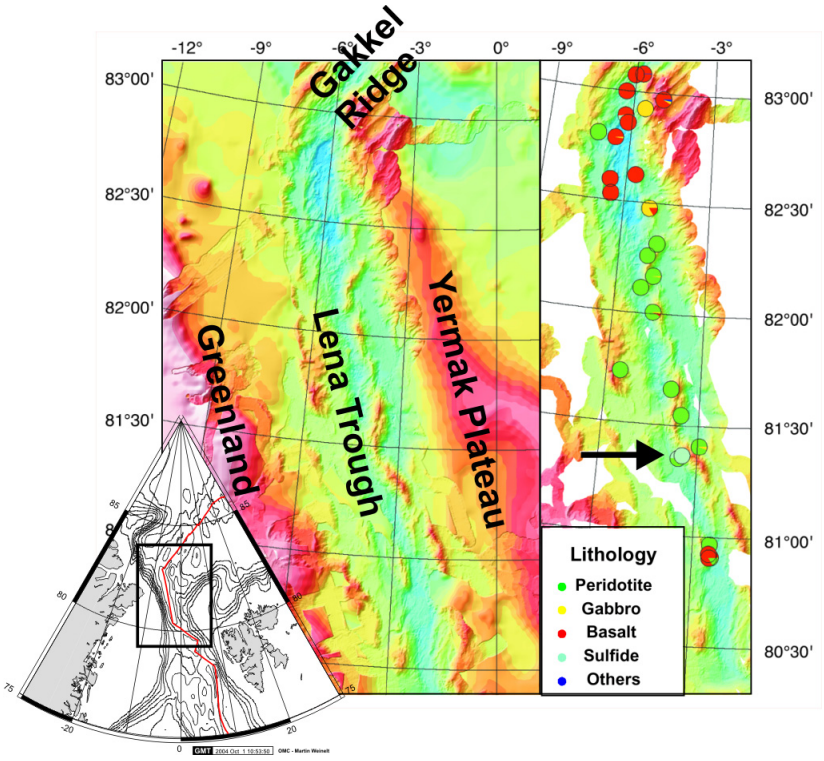

Fig. 1

Nauret and Snow

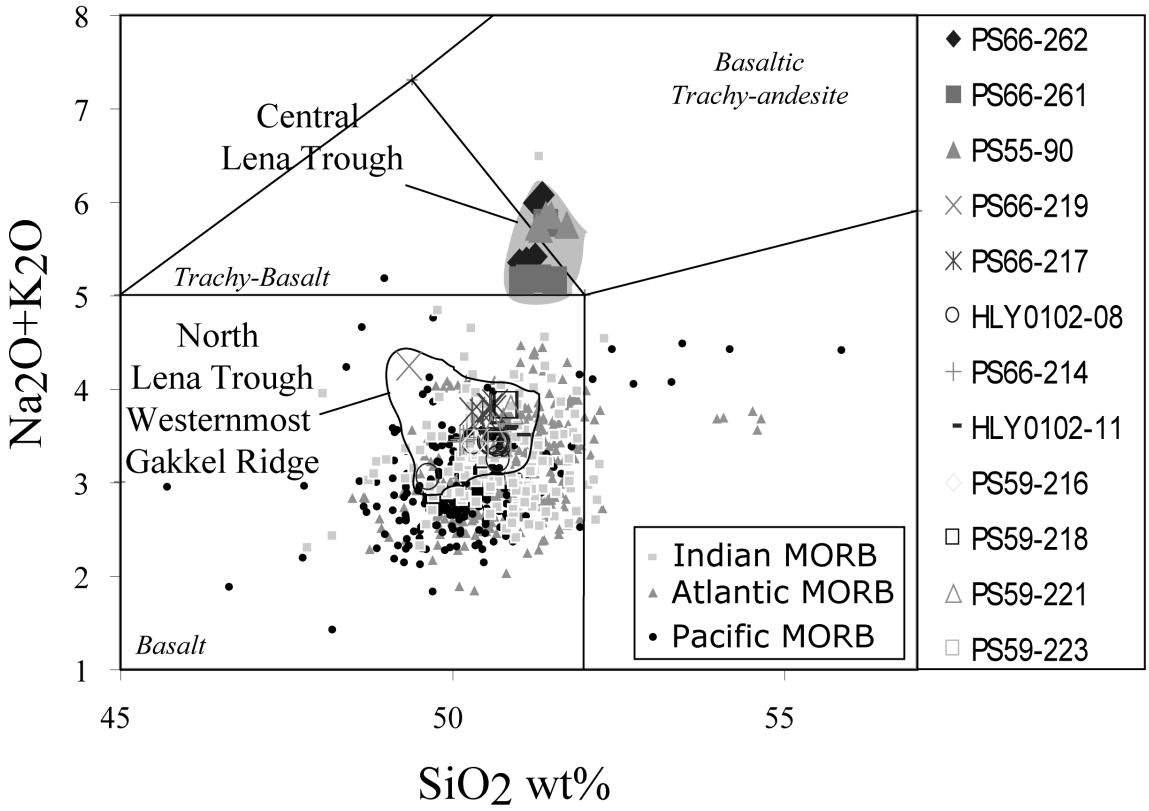

Fig. 2
Nauret and Snow

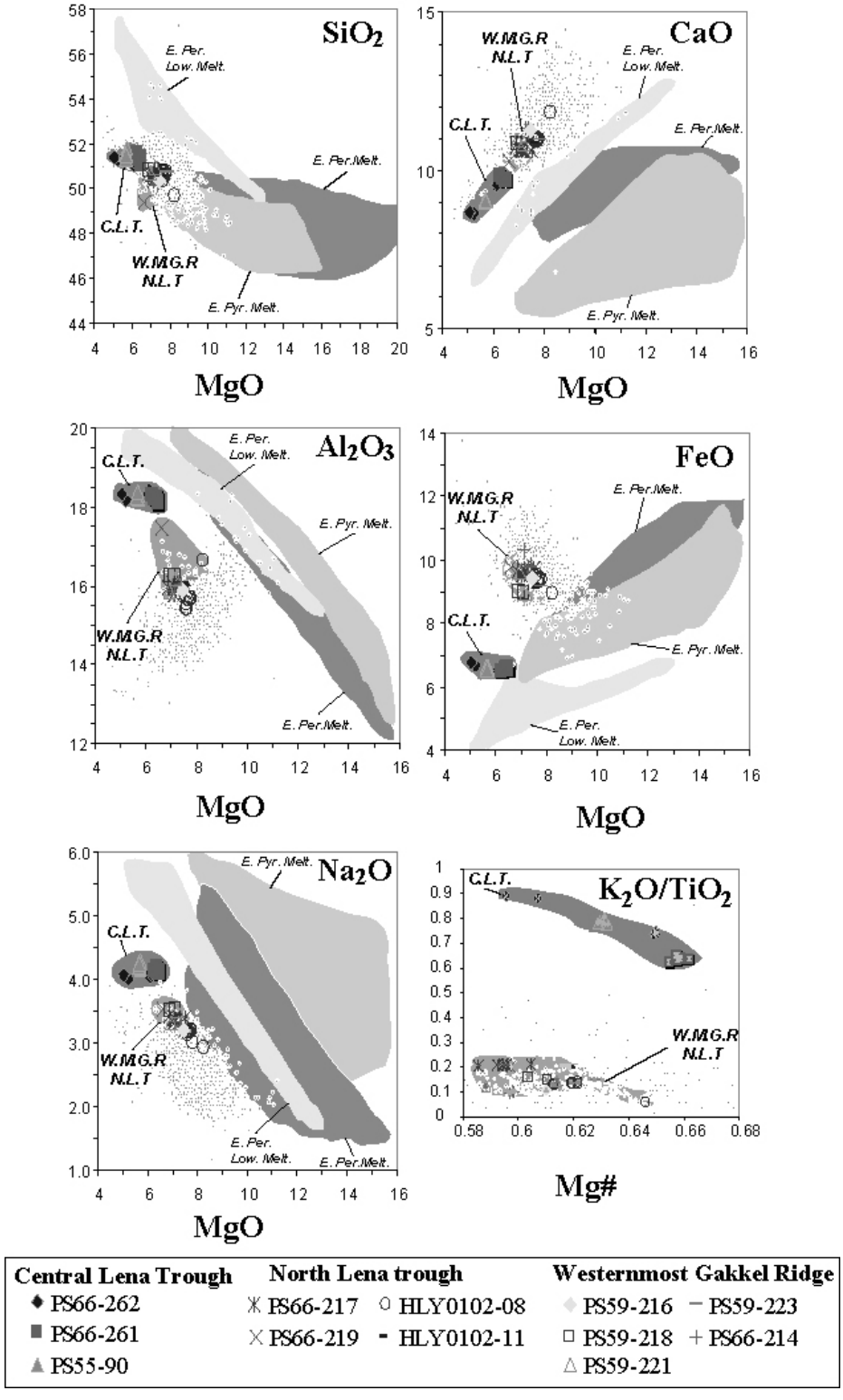

Fig. 3
Nauret and Snow

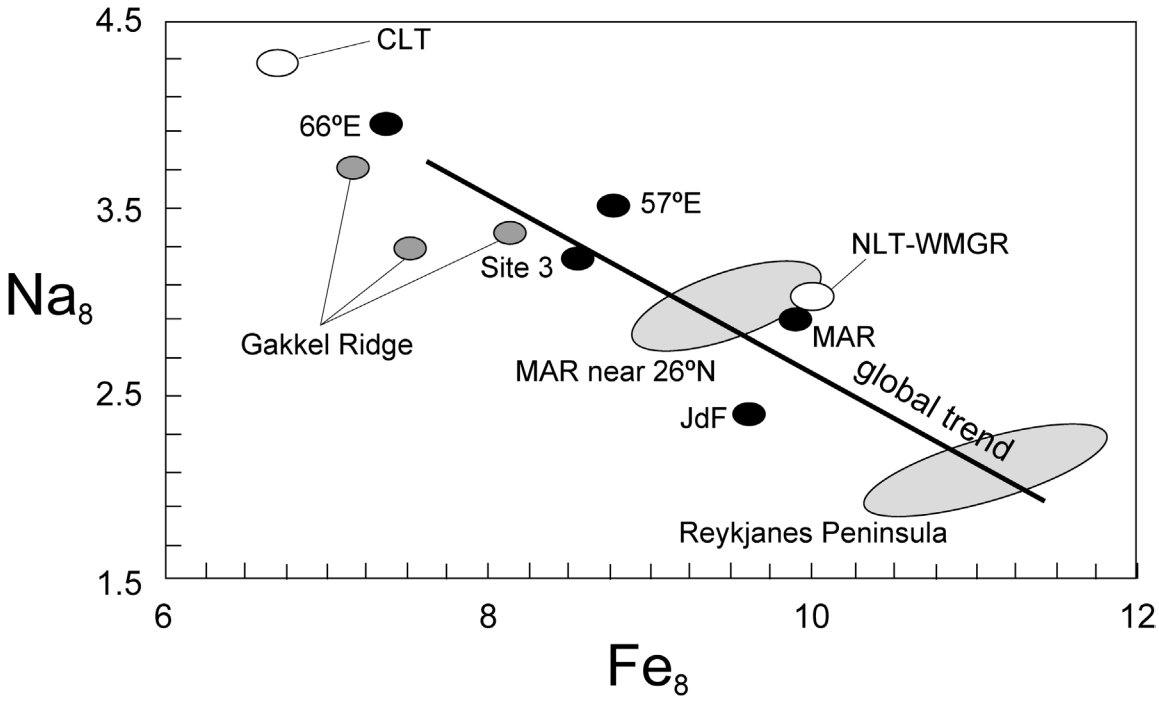

Fig. 4
Nauret and Snow

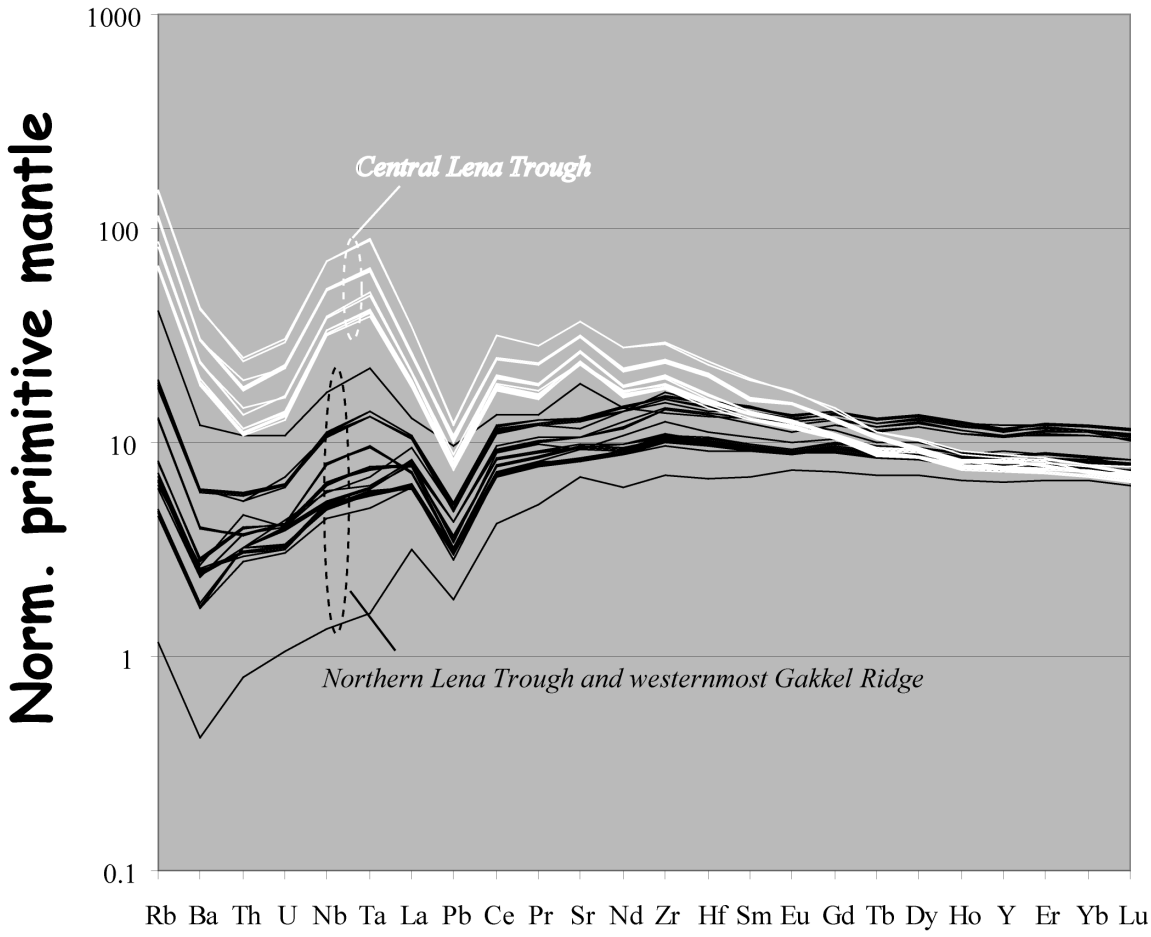

Fig. 5
Nauret and Snow

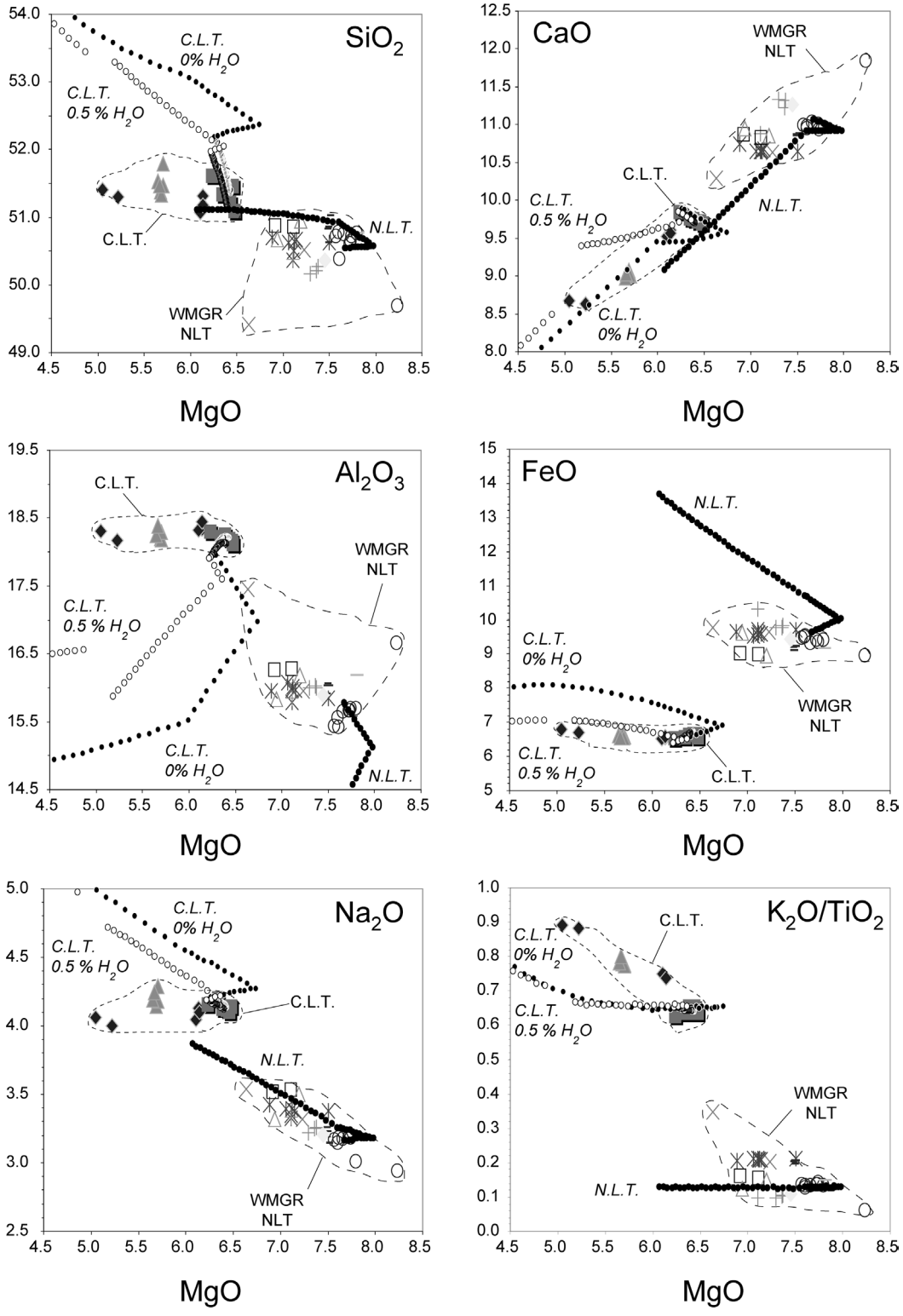

Fig. 6

Nauret and Snow

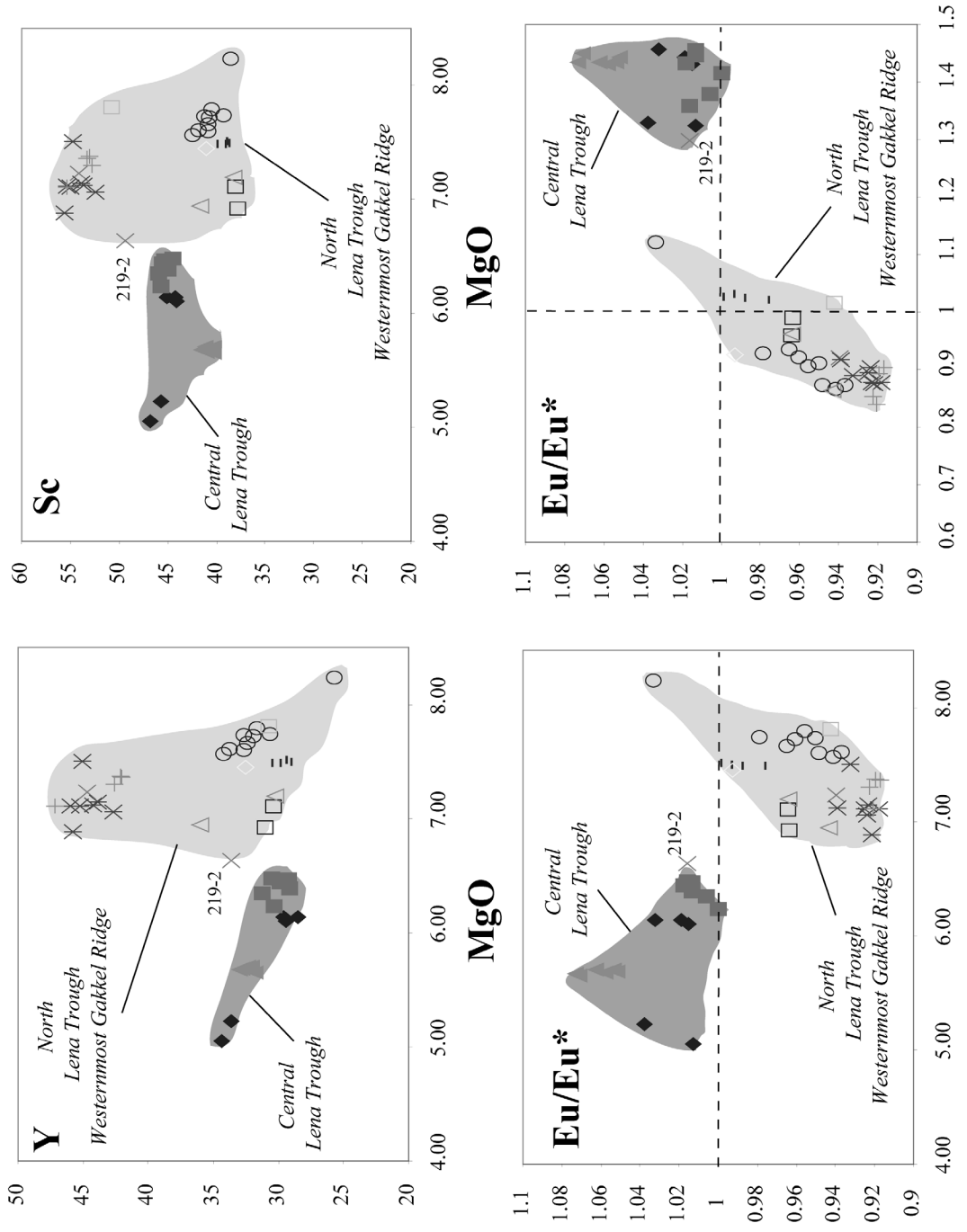

Fig. 7
Nauret and Snow

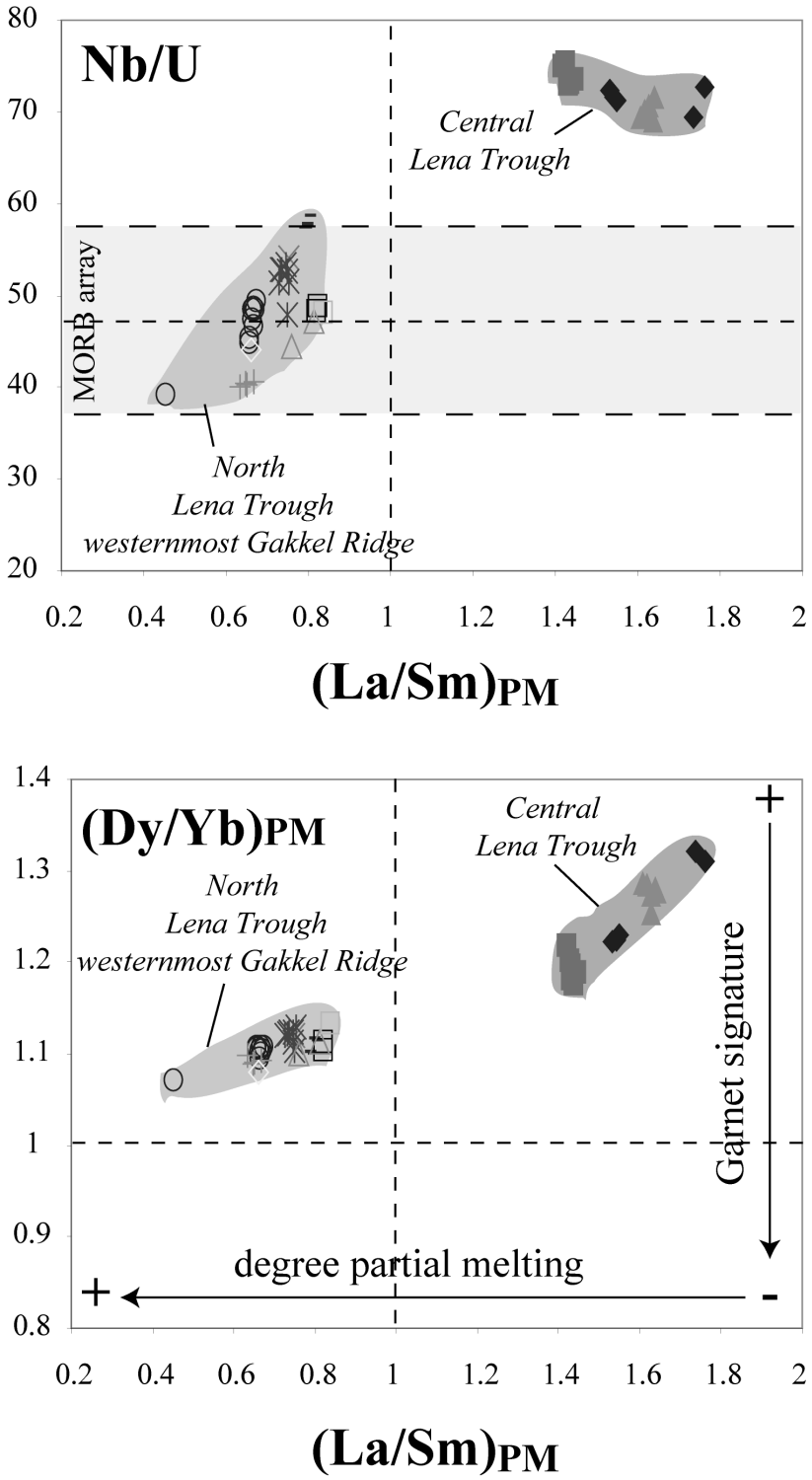

Fig. 8
Nauret and Snow

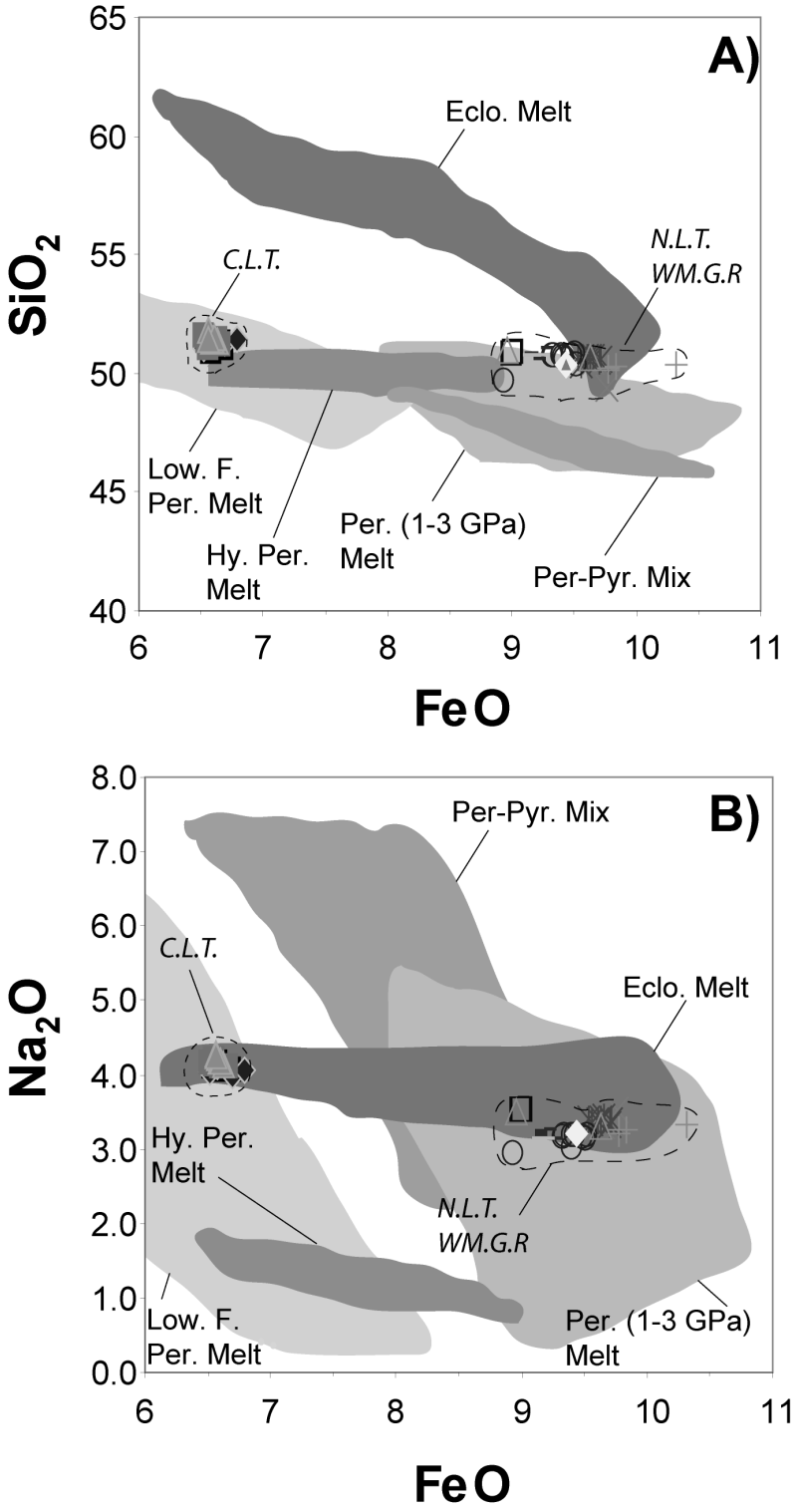

Fig. 9
Nauret and Snow

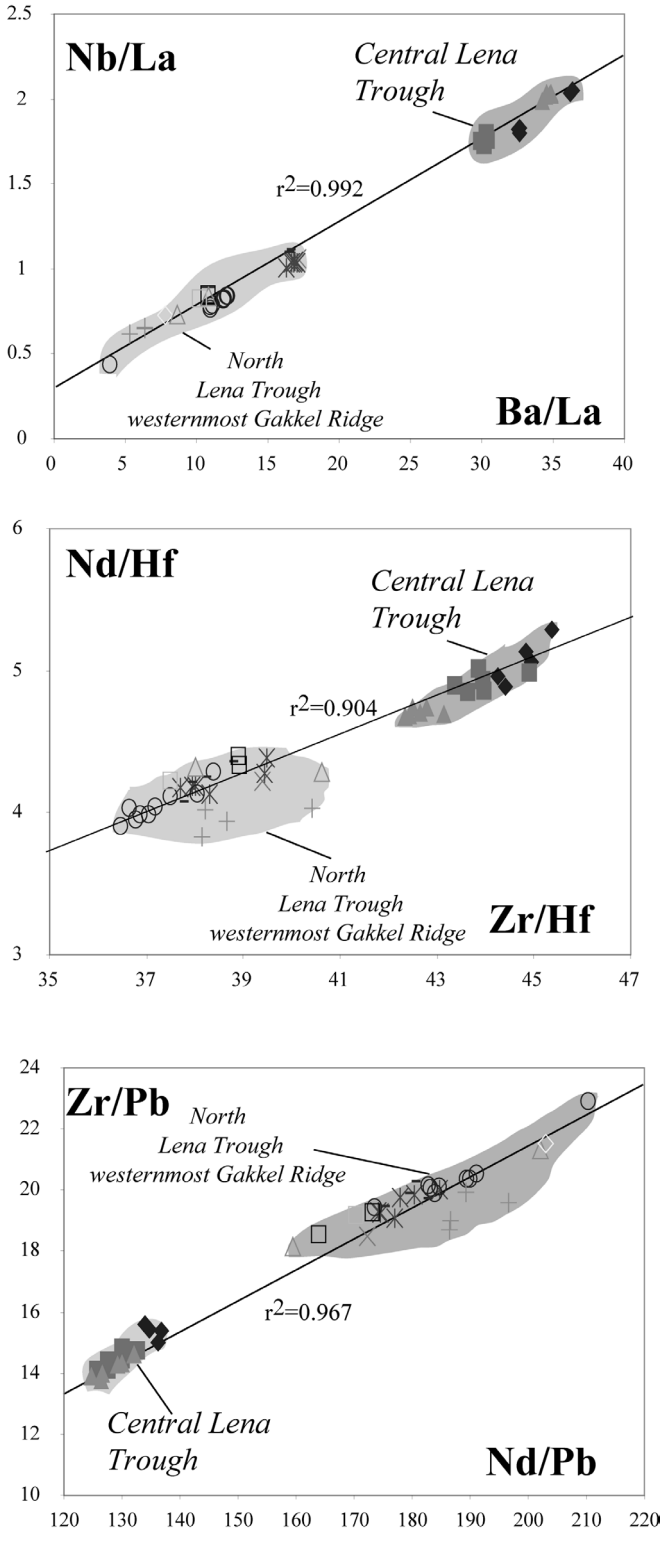

Fig. 10
Nauret and Snow

References:

[1] D.A. Wood, J.L. Joron, M. Treuil, M. Norry, J. Tarney, Elemental And Sr Isotope Variations In Basic Lavas From Iceland And The Surrounding Ocean-Floor - Nature Of Mantle Source Inhomogeneities, Contrib. Mineral. Petrol. 70(1979) 319-339.

[2] A.W. Hofmann, S.R. Hart, An assessment of local and regional isotopic equilibrium in the mantle, Earth Planet. Sci. Lett. 39(1978) 44-62.

[3] A.P. Leroex, A.J. Erlank, H.D. Needham, Geochemical And Mineralogical Evidence For The Occurrence Of At Least 3 Distinct Magma Types In The Famous Region, Contrib. Mineral. Petrol. 77(1981) 24-37.

[4] A.P. LeRoex, H.J.B. Dick, R.T. Watkins, Petrogenesis Of Anomalous K-Enriched Morb From The Southwest Indian Ridge - 11°53E To 14°38'E, Contrib. Mineral. Petrol. 110(1992) 253-268.

[5] V.J.M. Salters, H.J.B. Dick, Mineralogy of the mid-ocean-ridge basalt source from neodymium isotopic composition of abyssal peridotites, Nature 418(2002) 68-72.

[6] J.E. Snow, S.R. Hart, H.J.B. Dick, Nd And Sr Isotope Evidence Linking Mid-Ocean-Ridge Basalts And Abyssal Peridotites, Nature 371(1994) 57-60.

[7] I. Reid, H.R. Jackson, Oceanic Spreading Rate And Crustal Thickness, Marine Geophysical Researches 5(1981) 165-172.

[8] J.W. Bown, R.S. White, variation with spreading rate of oceanic crustal thickness and geochemistry, Earth Planet. Sci. Lett. 121(1994) 435-449.

[9] E. Hellebrand, J.E. Snow, Deep melting and sodic metasomatism underneath the highly oblique-spreading Lena Trough (Arctic Ocean), Earth Planet. Sci. Lett. 216(2003) 283-299.

[10] P.J. Michael, C.H. Langmuir, H.J.B. Dick, J.E. Snow, S.L. Goldstein, D.W. Graham, K. Lehnert, G. Kurras, W. Jokat, R. Muhe, H.N. Edmonds, Magmatic and amagmatic seafloor generation at the ultraslow-spreading Gakkel ridge, Arctic Ocean, Nature 423(2003) 956-U951.

[11] J.E. Snow, H.J.B. Dick, E. Hellebrand, A. Buchl, A. von der Handt, C. Langmuir, P. Michael, Geochemistry of abyssal peridotites from Gakkel Ridge, Arctic Ocean, Geochim. Cosmochim. Acta 66(2002) A722-A722.

[12] H.J.B. Dick, J. Lin, H. Schouten, An ultraslow-spreading class of ocean ridge, Nature 426(2003) 405-412.

[13] J.E. Snow, W. Jokat, E. Hellebrand, R. Muhe, Magmatic and Hydrothermal activity in Lena Trough, Arctic Ocean, EOS Trans. AGU 82(2001).

[14] J.E. Snow, Petrology-Group-ARK-XX-2, Petrology of Lena Trough and Gakkel Ridge, Reports on Polar and Marine Research in press(2006).

[15] M.J. Le Bas, A.L. Streckreisen, The IUGS systematic of igneous rocks, J. Geol. Soc. London 148(1991) 825-833.

[16] E.M. Klein, C.H. Langmuir, Global Correlations of Ocean Ridge Basalt Chemistry with Axial Depth and Crustal Thickness, J. Geophys. Res. 92(1987) 8089-8115.

[17] C.H. Langmuir, E.M. Klein, T. Plank, Petrological Systematics of Mid-Ocean Ridge Basalts: Constraints on Melt Generation Beneath Ocean Ridges, in: A.G. Union, (Ed), Mantle Flow and Melt Generation at Mid-Ocean Ridges Geophysical Monograph 71, 1992.

[18] M.M. Hirschmann, T. Kogiso, M.B. Baker, E.M. Stolper, Alkalic magmas generated by partial melting of garnet pyroxenite, Geology 31(2003) 481-484.

[19] P.J. Michael, C.H. Langmuir, S. Goldstein, G. Soffer, H. Dick, J.E. Snow, D. Graham, Geochemistry of Gakkel Ridge, Geochim. Cosmochim. Acta 68(2004) A692-A692.

[20] A.W. Hofmann, Chemical differentiation of the Earth: the relationship between mantle, continental crust, and oceanic crust., Earth Planet. Sci. Lett. 90(1988) 297-314.

[21] M.S. Ghiorso, Algorithms for the estimation of phase-stability in heterogeneous thermodynamic systems, Geochim. Cosmochim. Acta 58(1994) 5489-5501.

[22] K. Hirose, K. Kawamura, A New Experimental Approach for Incremental Batch Melting of Peridotite at 1.5-Gpa, Geophysical Research Letters 21(1994) 2139-2142.

[23] M.J. Walter, Melting of Garnet Peridotite and the Origin of Komatiite and Depleted Lithopshere, J. Petrol 39(1998) 29-60.

[24] K. Hirose, I. Kushiro, Partial Melting of Dry Peridotites at High-Pressures - Determination of Compositions of Melts Segregated from Peridotite Using Aggregates of Diamond, Earth Planet. Sci. Lett. 114(1993) 477-489.

[25] Y. Niu, M. Regelous, J.I. Wendt., R. Batiza, M.J. O'Hara, Geochemistry of near-EPR seamounts: importance of source vs. process and the origin of enriched mantle component, Earth Planet. Sci. Lett. 199(2002) 327-345.

[26] M.B. Baker, M.M. Hirschmann, M.S. Ghiorso, E.M. Stolper, Compositions of

near-solidus peridotite melts from experiments and thermodynamic calculations, Nature 375(1995) 308-311.

[27] T.J. Falloon, D.H. Green, H.S.C. O'Neill, W.O. Hibberson, Experimental tests of low degree peridotite patial melt compositions: implications for the nature of anhydrous near-solidus peridotite melts at 1GPa, Earth Planet. Sci. Lett. 152(1997) 149-162.

[28] S. Villiger, P. Ulmer, O. Muentener, A.B. Thompson, The Liqui Line of Descent of Anhydrous, Mantle-Derived, Tholeiitic Liquids by Fractional and Equilibrium Crystallization-an Experimental Study at 1.0 GPa, J. Petrol 45(2004) 2369-2388.

[29] D. Laporte, M.J. Toplis, M. Seyler, J.-L. Devidal, A new experimental technique for extracting liquids from peridotite at very low degrees of melting: application to partial melting of depleted peridotite, Contrib. Mineral. Petrol. 146(2004) 463-484.

[30] K. Hirose, T. Kawamoto, Hydrous Partial Melting of Iherzolite at 1 Gpa - the Effect of H_2O on the Genesis of Basaltic Magmas, Earth Planet. Sci. Lett. 133(1995) 463-473.

[31] M.M. Hirschmann, M.S. Ghiorso, L.E. Wasylenki, P.D. Asimow, E.M. Stolper, Calculation of peridotite partial melting from thermodynamic models of minerals and melts. I. Review of methods and comparison with experiments, J. Petrol 39(1998) 1091-1115.

[32] M.M. Hirschmann, E.M. Stolper, A possible role for garnet pyroxenite in the origin of the "garnet signature" in MORB, Contrib. Mineral. Petrol 124(1996) 185-208.

[33] T. Kogiso, M.M. Hirschmann, M. Pertermann, High-pressure Partial Melting of Mafic Lithologies in the Mantle, J. Petrol 45(2004) 2407-2422.

[34] M. Pertermann, M.M. Hirschmann, Partial melting experiments on a MORB-like pyroxenite between 2 and 3 GPa: constraints on the presence of pyroxenite in basalt source regions from solidus location and melting rate, J. Geophys. Res. 108(2003) 2125-2143.

[35] M. Pertermann, M.M. Hirschmann, Anhydrous Partial Melting Experiments on MORB-like Eclogite: Phase Relations, Phase Compositions and Mineral-Melt Partitioning of Major Elements at 2-3 GPa, J. Petrol 44(2003) 2173-2201.

[36] G.M. Yaxley, Experimental study of the phase and melting relations of homogeneous basalt + peridotite mixtures and implications for the petrogenesis of flood basalts, Contrib. Mineral. Petrol 139(2000) 326-338.

[37] G.M. Yaxley, D.H. Green, Reactions between eclogite and peridotite: mantle

refertilisation by subduction of oceanic crust., Schweiz Mineral Petrogr Mitt 78(1998) 243-255.

[38] Sobolev A.V., Hofmann A.W., S.V. Sobolev, I.K. Nikogosian, An Olivine-free mantle source of Hawaiian shield basalt, Nature 434(2005) 590-597.

[39] A. Yasuda, T. Fujii, K. Kurita, Melting phase relations of an anhydrous mid-ocean ridge basalt from 3 to 20 GPa: implications for the behavior of subducted oceanic crust in the mantle, J. Geophys. Res. 99(1994) 9401-9414.

[40] C. Li, E.M. Ripley, E.A. Mathez, The effect of S on the partitioning of Ni between olivine and silicate melt in MORB, Chem. Geol. 201(2003) 295-306.

[41] T. Kogiso, K. Hirose, E. Takahashi, Melting experiments on homogeneous mixtures of peridotite and basalt: application to the genesis of ocean island basalts, Earth Planet. Sci. Lett. 162(1998) 45-61.

[42] K.E. Donnelly, S.L. Goldstein, C.H. Langmuir, M. Spiegelman, Origin of enriched ocean ridge basalts and implications for mantle dynamics, Earth Planet. Sci. Lett. 226(2004) 347-366.

[43] J. Blichert-Toft, A. Agranier, M. Andres, R. Kingsley, J.G. Schilling, F. Albarède, Geochemical segmentation of the Mid-Atlantic Ridge north of Iceland and ridge-hot spot interaction in the North Atlantic, Geochem. Geophys. Geosyst. 6(2005). doi: 10.1029/2004GC000788

[44] C.H. Langmuir, R.D. Vocke, H. G.N., S.R. Hart, A general mixing equation with applications to icelandic basalts, Earth Planet. Sci. Lett. 37(1978) 380-392.

[45] C.J. Allègre, D.L. Turcotte, Implications of a two-component marble-cake mantle, Nature 323(1986) 123-127.

[46] C.J. Robinson, M.J. Bickle, T.A. Minshull, R.S. White, A.R.L. Nichols, Low degree melting under the Southwest Indian Ridge: the roles of mantle temperature, conductive cooling and wet melting, Earth Planet. Sci. Lett. 188(2001) 383-398.

[47] E.T. Baker, H.N. Edmonds, P.J. Michael, W. Bach, H.J.B. Dick, J.E. Snow, S.L. Walker, N.R. Banerjee, C.H. Langmuir, Hydrothermal venting in magma deserts: The ultraslow-spreading Gakkel and Southwest Indian Ridges, Geochemistry Geophysics Geosystems 5(2004). doi:10.1029/2004GC000712